UNIVERSITA' DEGLI STUDI DI TORINO

DIPARTIMENTO DI SCIENZE DELLA SANITÀ PUBBLICA E PEDIATRICHE

DOTTORATO DI RICERCA IN SCIENZE BIOMEDICHE ED ONCOLOGIA

CICLO: 35°

TITOLO DELLA TESI: Tumour Genomic Profile Analysis in Children, Adolescents and Young Adults With Bone Sarcomas: a national multi-centre prospective trial.

TESI PRESENTATA DA: dott.ssa Elisa Tirtei

TUTORS: Prof.ssa Franca Fagioli, Prof. Giovanni Battista Ferrero

COORDINATORE DEL DOTTORATO: Prof. Emilio Hirsch

ANNI ACCADEMICI: 2019-2023

SETTORE SCIENTIFICO-DISCIPLINARE DI AFFERENZA: MED-038

TURIN UNIVERSITY

DEPARTMENT OF SCIENCES OF PUBLIC HEALTH AND PEDIATRICS

Ph.D. PROGRAM IN BIOMEDICAL SCIENCES AND ONCOLOGY

CYCLE: 35th

THESIS TITLE: Tumour Genomic Profile Analysis in Children, Adolescents and Young Adults With Bone Sarcomas: a national multi-centre prospective trial.

Ph.D. STUDENT: dr Elisa Tirtei

TUTORS: Prof. Franca Fagioli, Prof. Giovanni Battista Ferrero

Ph.D. PROGRAM COORDINATOR: Prof. Emilio Hirsch

ACADEMIC YEARS: 2019-2023

SCIENTIFIC AREA: MED-038

"I've always thought that the first gift that the patient must have from the doctor is the gift of science, the gift of being treated as it goes."

Giancarlo Rastelli MD
(Parma University-Mayo Clinic)

SUMMARY

TITLE

Tumour Genomic Profile Analysis in Children, Adolescents and Young Adults With Bone Sarcomas: a national multi-centre prospective trial.

INTRODUCTION

High-Grade Osteosarcoma (HOS) and Ewing sarcoma (EWS) are the two most common bone sarcomas (BS) in the paediatric population and they represent two heterogeneous diseases with distinct clinical, genomic and pathologic traits (1)(2)(3)(4). Advanced or relapsed/refractory HOS and EWS continue to constitute a significant challenge in cancer therapy, due to their resistance to chemotherapy and consequent poor survival rates (5).

Over the last few decades, the availability of next-generation sequencing (NGS) techniques have exploited the omic sciences, allowing the study of complex biological systems such as cancer at different molecular levels (4)(6). The employment of multi-omic NGS approaches is crucial in order to better understand the molecular processes that characterise heterogeneous cancer types such as BS, to improve diagnostic accuracy, to potentially find a new efficacy within therapeutic targets, and to contribute to improve the knowledge about the carcinogenesis process.

In this context, SAR-GEN2016 and SAR-GEN_ITA are the two first national prospective trials entirely devoted to evaluating the genomic profile analyses of BS in children, adolescents and young adults for clinical and research purposes.

This thesis aims to describe the wide translational research approach of SAR-GEN projects with the dual goals of integrating the NGS data into therapeutical decision-making for each enrolled patient and studying the biological and genomic process involved in HOS carcinogenesis.

MATERIALS AND METHODS

Patients and biological specimens

All clinical data and biological samples were collected within the clinical trials entitled "Genomic Profile Analysis in Children, Adolescents and Young Adults with Sarcomas – SAR-GEN_ITA" (ClinicalTrials.gov ID: NCT04621201) and the Pilot Study SAR-GEN2016. The trials were approved by the local independent ethics committee of all AIEOP (Italian Association of Paediatric Onco-Haematology) Centres involved, and they were conducted according to the principles of the Declaration of Helsinki and Good Clinical Practice. Informed written consent was obtained from each subject or guardian.

The following eligibility criteria were set: i) patients with a suspected first diagnosis or recurrence of sarcoma (patients with HOS and EWS were analyzed for this thesis) ii) age < 40 years; iii) fresh tumour sample or formalin fixed paraffin embedded (FFPE) tumour block available; iv) peripheral blood (10 ml EDTA tube) available; v) confirmatory diagnosis validated through rigorous pathological examination by a local or national pathologist. The study included FFPE blocks non-decalcified or decalcified (a specific method of decalcification was not required) and only FFPE blocks with at least 20% of tumor content were included.

Fresh tumour samples and peripheral blood tubes were centralized within 48 hours from their collection to Regina Margherita Children's Hospital Laboratory and they were immediately processed for genomic analysis. Clinical Data and Histological features were recorded in specific Case Report Forms (CRFs). Clinical details collected included patients' features (sex, age, clinical history), sampling details (anatomical site of biopsy or surgical procedure), radiological and histological features of tumor mass and clinical follow-up.

Five healthy bone samples were collected from five patients enrolled in the trial for the tumour genomic analysis validation.

DNA extraction and whole exome sequencing

Genomic DNA from the tumour was extracted from 10 µm-thick FFPE sections (3–6 sections per sample) using Maxwell® RSC DNA FFPE Kit (Promega Corporation) on Maxwell® RSC 48 Instrument (Promega Corporation) following the manufacturer's protocol; or the genomic DNA was extracted from a fragment of fresh tumour sample using a QIAcube with DNeasy Blood and Tissue Kit, following the manufacturer's protocol. Peripheral blood was used as a matching reference. For five patients with HOS, healthy bone samples were collected during surgical procedures as an additional matching reference. DNA from blood samples was extracted with a QIAamp DNA Blood Kit (QIAGEN) following the manufacturer's protocol. Whole exome was captured from genomic DNA for tumour and matched normal samples using the SureSelect XT Human All Exon V6 + COSMIC (Agilent) and following the manufacturer's protocol as previously described (7). Briefly, 0.2 µg of genomic DNA was subjected to hydrodynamic shearing by exposure to 3 minutes of sonication using a Covaris sonicator to obtain ~200-bp-long fragments. Fragments were used to prepare libraries according to the SureSelect XT manual. Libraries were further amplified with 7–10 cycles of PCR, and 150 ng were hybridised with the bait library. Captured DNA was amplified with 14 PCR cycles and barcode indexes were added. Libraries were sequenced using Illumina NovaSeq6000 in 150nt-long paired-end modality.

Sequence alignment and variant calling

Somatic mutations were identified integrating a previously published pipeline (7) according to the GATK Best Practice guidelines as implemented in the HaTSPiL framework (8). In particular, sequencing reads from each sample were aligned to the human genome reference (GRCh37/hg19) using Novoalign (http://www.novocraft.com/) with default parameters. A maximum of three mismatches per read were allowed, and PCR duplicates were removed using the Picard Markduplicates tool (9). To improve accuracy of variant calling, local realignment around indels was performed using GATK RealignerTargetCreator and IndelRealigner tools. Single nucleotide variants (SBSs) and small insertion/deletions (IDs) were identified using MuTect v.1.1.17(10), Strelka v.1.0.15 (11), and Varscan2 v.2.3.6 (12) in tumour and normal samples independently. Only variants identified as 'KEEP' and 'PASS' in MuTect and Strelka, respectively, were considered. SBSs and InDels were retained if they (i) had allele frequency ≥5% and (ii) were in a genomic position covered by at least 10 reads.

Identification of inherited genomic aberration

Frequency distributions of the germline SNVs and InDels identified by varscan2 were inspected. To identify relevant germline mutations, we selected variants that harbour an allele frequency ≥25%. Clinical interpretation of germline mutations was derived from ClinVar database (https://www.ncbi.nlm.nih.gov/clinvar/) and InterVar (13), which follows ACMG2015 guidelines (14), as previously described (15). Variants that were classified as "Pathogenic" or "Likely Pathogenic" by at least one database were kept for further analyses.

Copy number detection

Somatic CNV regions were identified using Sequenza v.3.0.0 (16) with parameters window=5mb and min.reads.baf=4, retaining only positions that were covered by at least 10 reads. A gene was

considered as modified if ⩾80% of its length was contained in an aberrant region. To identify regions of recurrent copy number variations, GISTIC2 (17) analysis was carried out. In particular, Sequenza's segment copy number values were used as input and a confidence of 0.95 was required to consider a region as statistically significantly recurrent. GISTIC2 results were further filtered using an FDR value of 0.1. Gene annotations were also retrieved, and genes classified as cancer drivers according to the Network of Cancer Genes v.5 (18) (http://ncg.kcl.ac.uk/) were extracted for further inspection.

Identification of cancer driver mutations

In the tumour sample, SBSs and InDels from the three different tools were identified as somatic if not retrieved in the normal counterpart. ANNOVAR (19) was used to annotate variants. Non-silent (i.e. non-synonymous, stop-gain, stop-loss, frameshift, non-frameshift and splicing modifications) mutations according to the RefSeq v.64 (http://www.ncbi.nlm.nih.gov/RefSeq/) protein dataset were selected. SBSs and InDels falling within 2 bp from the splice sites of a gene were considered as splicing mutations. A list of cancer genes was then retrieved from the Network of Cancer Genes v.5 (18) (http://ncg.kcl.ac.uk/). Of these, 23 and 63 were extracted as paediatric and adult sarcoma driver genes, respectively (Supplementary Table 1). Furthermore, a list of 164 genes with actionable alterations was collected from the 'PrecisionTrialDrawer' R package (20) and considered as actionable genes (Supplementary Table 2). Variants were furtherly annotated using these two gene lists. All non-silent mutations and frameshift substitutions were retained if (i) identified by at least two variant callers or (ii) in genes annotated as cancer driver and/or actionable. Tumour Mutational Burden was calculated weighting the number of selected mutations over one-million normalised exome length.

Mutational and CNV signature analysis

Mutational signature analyses were performed on all somatic variations using SigProfilerMatrixGenerator (21) and SigProfilerExtractor (22), as previously described (23). Copy Number Alteration burden was evaluated using the read_copynumber function from 'sigminer' (24)(25).

Total RNA extraction and sequencing

Total RNA extracted from tumour biopsy using the RSC RNA FFPE Kit or RNeasy Protect Mini Kit (250 - Qiagen) on Maxwell instrument. To exclude genomic contamination, total RNA was treated with DNAse I and cleared with RNA Clean and Concentration (Zymo Research). RNA quantity and quality were determined by Qubit Fluorometric Quantitation (Thermo Fisher Scientific) and use of the RNA 6000 Nano kit on a Bioanalyser (Agilent Technologies), respectively. RNA-seq libraries were generated from 0.1 µg of RNA using Illumina Total RNA Prep Stranded Ligation with Ribo-Zero according to manufacturer's recommendations, and sequenced on Illumina NovaSeq6000 in 100nt-long paired-end read modality.

Expression analyses of RNA-seq data

Raw sequencing reads were trimmed to avoid nucleotide overlaps between read pairs on both ends using the bbduck tool from bbmap (26) v.38.18 with parameters forcetrimright=50 and minlength=30. Trimmed reads were aligned to the human genome reference GENCODE GRCh38 version 33 (27) using STAR v.2.7.3a 76 in basic two-pass mode removing duplicates and preventing multimappings (i.e. --bamRemoveDuplicatesType UniqueIdentical and --outFilterMultimapNmax 1). Moreover, the following parameters were used: --alignInsertionFlush Right --outSAMstrandField intronMotif --

outSAMattributes NH HI NM MD AS XS --peOverlapNbasesMin 20 --peOverlapMMp 0.25 --chimSegmentMin 12 --chimJunctionOverhangMin 8 --chimOutJunctionFormat 1 --chimMultimapScoreRange 3 --chimScoreJunctionNonGTAG -4 --chimMultimapNmax 20 and --chimNonchimScoreDropMin 10. Gene fusions were identified using STAR-Fusion v. 1.9.0 with options --min_FFPM 0 --FusionInspector validate --examine_coding_effect. Only fusions (FFPM≥0.1, LargeAnchorSupport="YES", LeftBreakEntropy≥1 and RightBreakEntropy≥1) were retained for further analysis. Read counts at gene level were estimated using featureCounts from Subread v. 2.0.0 77 with parameters -O --primary -Q 1 -J -s 2 -p -B.

Differential expression analysis

A DeSeq2 differential gene expression workflow was followed, as previously carried out (28). In particular, two analyses were performed, i.e. HOS versus normal bone samples, and metastatic versus localised HOS.

For the first analyses, given the difference in numerosity between cases and controls, a Monte Carlo simulation was required. Empirical p-values and success rates were evaluated, as previously performed (28). Genes that were significantly differentially expressed (DE) according to DeSeq2 analysis (padj≤0.001 and absolute log2FoldChange≥1) and presented an empirical pvalue ≤ 0.001 and a success rate ≥ 0.7 were selected as high-confidence DE genes and used for further considerations.

For the second analyses, given the balanced numerosity of cases and controls, DE genes were selected only for presenting padj≤0.1 and absolute log2FoldChange≥1.

Over-representation analysis

Over-representation analyses were performed with the enricher function in the R package 'clusterProfileR' (29)(30) using the 50 Hallmark gene sets defined in the mSigDb (31) and available through the R package 'msigdbr'. Terms with p.adjust≤0.1 were considered as significantly enriched.

Molecular Tumour Board

As previously reported in other international genomic profiling programmes (32)(33)(34)(35), the Multidisciplinary Tumour Board reported somatic or germline genomic alterations as "potentially actionable" when the identified molecular lesion would be theoretically targetable by an investigational or approved drug, either directly or indirectly in the affected pathway. To better define the targets, the ESMO Scale for Clinical Actionability of molecular Targets (ESCAT) was considered (36). A clinical report with the list of the genomic findings and a therapeutical recommendation, when available, was done for each patient and it was delivered to the local investigator.

Statistical Analysis

The distribution of clinical and demographic characteristics of the patients are described with the median and inter-quantile ranges for the continuous variables and frequencies, and percentages for the categorical items. Comparisons of qualitative variables were conducted utilising the χ^2 test and Fisher's exact test when appropriate. The analysis of Overall Survival (OS) was conducted using the Kaplan-Meier method with a 95% confidence interval (95% CI). Differences between survival curves were tested through Log-rank tests. The level of statistical significance is set at a value of 0.05. Statistical analyses were performed using R software version 4.2.1 and STATA v 17.0.

RESULTS

Patient and Procedure Characteristics

From January 2017 to August 2023, 179 patients were enrolled among 15 AIEOP centres. Tumour materials at different disease timepoints were collected from five patients (diagnosis and first or subsequent recurrences) for a total of 186 samples.

All patients underwent a biopsy or surgical tumour resection and blood sampling as study procedure for tissue collection. All the procedures were performed as clinical practice and not specifically for the trial.

132 fresh samples (71%) were collected, 38 samples (20.5%) were FFPE blocks and 16 samples (8.5%) were used in their entirety for diagnostic purposes by the local pathologist, and a screening failure was performed.

Figure 1 describes the detailed study flow. 133 patients were affected by sarcomas and were officially included in the trials (total samples:140).

The median age at inclusion was 14 years old (range (0-71 years) and 101 patients (76%) were younger than 18 years old. 77 specimens were collected at first diagnosis and 63 at recurrence.

Main sarcoma histo-types were BS: 48 patients with Osteosarcoma (HOS) (36%) and 40 patients with Ewing Sarcoma (EWS) (30%). Other sarcoma type distribution is detailed in Figure 2.

For this analysis, only HOS and EWS samples were considered (total: 94 specimens with 50 HOS and 44 EWS)

The Whole Exome Sequencing (WXS) was successfully carried out for 76 samples (57 fresh and 19 FPPE samples) (success rate: 81%), and RNA-Sequencing was successfully carried out for 68 samples (51 fresh and 17 FPPE samples) (success rate: 74.7%).

The WXS success rate was statistically higher for fresh samples compared to FPPE samples: 63.7% vs 23% (p=0.042).

The RNA-Seq success rate was 18.6% and 56% for FPPE and fresh samples, respectively, not reaching a statistical significance (p=0.06).

The bone origin or disease type did not affect the success of WXS and RNA-Seq.

HOS Cohort: Patient and Sample Characteristics

Forty-eight patients with HOS were included in the trial and fifty HOS samples (for two patients, both 1st diagnosis and relapse samples were collected). 25 were male (52%) and 23 female (48%). The median age at study entry was 15 years old (range: 6-29 years) and the median follow-up from enrolment was 15.2 months (1-86 months). Clinical details are described in Table 1.

The Overall Survival (OS) was 80% [95% CI 68%, 94%], 74% [95% CI 61%, 89%] and 61% [95% CI 46%, 81%] at 12-, 18- and 24-months, respectively (Figure 3A). The OS was statistically different for patients enrolled at first diagnosis vs relapse and for localised vs metastatic patients. 12- and 18-months OS were respectively 90% [95% CI 80%, 100%] and 86% [95% CI 74%, 100%] for patients enrolled at first diagnosis vs 48% [95% CI 25%, 94%] and 36% [95% CI 15%, 87%] for relapsed patients ($X2$ (1, N = 48) = 17,3, Log-Rank $p < 0.01$) (Figure 3B). 18-months OS was respectively 87% [95% CI 74%, 100%] for localised patients vs 54% [95% CI 31%, 95%] for metastatic patients ($X2$ (1, N = 48) = 8,8, Log-Rank $p < 0.01$) (Figure 3C).

WXS and RNA-Seq were performed successfully for 40 samples, 1 sample was analysed only with WXS; 9 samples were not adequate for genomic analysis and they were excluded from the final analysis.
The WXS success rate was higher for fresh HOS samples compared to FFPE samples: 95% vs 55.5% (p=0.042), X2 (1, N = 50) = 10.94, p <0.01, OR 15.6 (CI 95% 1.59-195.27). Otherwise, the RNA-Seq success rate was not statistically different between fresh vs FFPE samples.
Sample characteristics are described in Table 2.

EWS Cohort: Patient and Sample Characteristics

Forty patients with EWS were included in the trial and 44 EWS samples were processed (for one patient, both first diagnosis and relapse samples were collected and four subsequent relapse samples of one patient were collected). 26 were male (65%) and 14 female (35%). The median age at study entry was 14 years old (range: 3-29 years) and the median follow-up from enrolment was 12 months (2-55 months). Clinical details are described in Table 3.

The Overall Survival (OS) was 62% [95% CI 48%, 82%], 44% [95% CI 30%, 67%] and 41% [95% CI 26%, 63%], at 12-, 18- and 24-months, respectively (Figure 3A). The OS was statistically different for patients enrolled at first diagnosis and relapse. 12- and 18-months OS were respectively 83% [95% CI 65%, 100%] and 75% [95% CI 54%, 100%] for patients enrolled at first diagnosis vs 49% [95% CI 31%, 78%] and 22% [95% CI 8.6%, 57%] for relapsed patients (X2 (1, N = 48) = 17.3, Log-Rank p <0.01) (Figure 3B). 18-months OS was respectively 87% [95% CI 74%, 100%] for patients with a localized disease vs 54% [95% CI 31%, 95%] for patients with a metastatic disease (X2 (1, N = 40) = 6.2, Log-Rank p =0.01) (Figure 3D).

WXS and RNA-Seq were performed successfully for 27 samples; 8 samples were analysed only with WXS; for 1 sample, only RNA-Seq was performed; and 8 samples were not adequate for genomic analysis and thus excluded from the final analysis.
The sample type (fresh vs FFPE) and sample origin (bone vs other) did not affect the genomic analysis quality in the EWS cohort.
Sample characteristics are described in Table 4.

Clinical Recommendation on genomic findings

Among 77 samples with a successfully WXS and/or RNA-Seq, a “potentially actionable” genomic target was identified in 45 samples (58.4%) from 45 patients (26 patients enrolled at first diagnosis and 19 patients enrolled at recurrence). Of 90 “potentially actionable” genomic findings, 5 were single-nucleotide variants (SNV; 4 somatic, 1 germline), 3 elevated tumour mutational load (> 10muts/Mb), 82 focal copy-number alterations (CAN, 65 amplifications and 17 deletions), no “actionable” gene fusions were identified. Details are reported in Figure 4 and 5.
Among 45 patients with at least one “potentially actionable” genomic alterations, three (6.5%) were treated with a matched therapy, representing the 15.7% of relapsed patients with one or more “potentially actionable” alteration (3/19 patients). All of them were patients affected by EWS and they received a target drug after the 3rd line of treatment. Two of them obtained an initial clinical benefit, then showed a progressive disease with *exitus*. For one patient, the treatment is still ongoing (more than one month) with a stable condition.

Nine patients did not receive any genomic matched treatment because of their deteriorated clinical conditions or unavailability of drugs in the country (Table 5).

The somatic genomic landscape of HOS cohort

Whole Exome Analysis revealed a low mutational burden and a high genomic instability

To assess the somatic alterations of HOS cohort samples, we sequenced the exome of the tumour and we identified single base substitutions (SBSs) and small insertions/deletions (IDs). We compared variant calling results between tumour and blood samples.

Overall, the SBS landscape of the tumour was characterised by a prevalence of C>T substitutions, followed by C>A substitutions (Figure 6). These mutational patterns were recapitulated by the known COSMIC SBS5 and SBS1 (Figure 7). SBS5 and SBS1 are both present in 94.8% of samples. They have been recurrently found in paediatric cancers (37). While SBS5 is of unknown aetiology, SBS1 is indicative of deamination of 5-methylcytosine (5mC) to thymine (37). The presence of distant metastasis and prognosis do not correlate with the presence or absence of a specific SBS type.

The combination of COSMIC signatures SBS1 and SBS5 matches with a *de novo* extracted signature SBS96A (Figure 8).

The ID signatures presented a more homogeneous distribution, mainly characterised by single base T insertions and deletions in long thymine homopolymers, as well as small deletions in repeated regions (Figure 9). This pattern recapitulated a combination of COSMIC ID1, ID2, and ID12 signatures. ID1 and ID2 defined the single base T insertions or deletions at T stretch repeats, whereas ID12 summarised the small deletions at repeated regions. Similarly to SBS1, ID1 and 2 have been recurrently found in paediatric cancers and associated with DNA damage induced by replication slippage (37). Although ID12 has been previously identified in pediatric patients with brain tumours (29), its etiology is unknown.

We then performed mutational signature extractions identifying the *de novo* extracted signature ID83A, which matches with ID2, ID12 and ID1 (Figure 10).

Furthermore, the mutational landscape was explored to identify possible driver alterations. We selected 'non-silent' alterations that were likely to impair the function of the encoded protein. These somatic variants accounted for a median tumour mutational burden of 0.61 muts/Mb (range: 0.17-2.49), which was in the range of genomic data previously reported (37) (38) (Figure 11A).

Out of a median value of 40 non-silent mutations per sample, no common mutations were identified across the whole HOS cohort. The most common alterations identified were missense mutation and SNV.

The mutational landscapes of HOS samples showed that the most commonly mutated genes are: MUC4, RB1, TTN, FLG, NOTCH2 and TP53 (Figure 12). However, these genes are commonly mutated in a very little cohort of patients (15-20%) demonstrating a wide mutational heterogeneity across HOS samples and patients.

Next, the chromosomal status of the tumour was assessed. By profiling CNA, the regions undergoing somatic alterations were identified. We found that 95% (range: 1.2%-100%) of the genome had undergone chromosomal changes (Figure 11B), demonstrating a high genomic instability of HOS samples, as previously reported in literature (38). Figure 13 describes the most commonly amplified

and deleted cytobands, and the most commonly amplified and deleted genes in the whole cohort are reported in Table 6.
The analysis of copy number (CN) signatures revealed that 56% of samples are enriched with CN18, 34% of samples are enriched with CN17, followed by CN20 (26.8%), CN14 and CN21 (14.5%) and CN9 (10%) (Figure 14).
Signature CN17 was previously reported in tumours described as being homologous recombination deficiency (HRD) and enriched in the tandem duplicator phenotype (23). In addition, it is also associated with increased hypoxia levels (39).
CN9 is a signature of chromosomal instability and chromothripsis, and it correlates with both deletion and duplication rearrangement classes (40). Moreover, it is associated with an increased hypoxia score from gene expression data (39).
CN14 is a chromosomal LOH signature, indicating chromosomal- or arm-scale losses before a whole genome doubling event (23). CN18, CN20 and CN21 are signatures of unknown origin.
We then performed signature extractions identifying the *de novo* extracted signature CNV48A, which matches with CN18 and CN20 (Figure 15).

RNA-Sequencing Analysis revealed a specific expression profile of metastatic HOS

Given the complex genomic landscape, we sought to investigate the transcriptomic profile of the HOS cohort. To do so, we extracted total RNA from tumour and healthy bone tissues and performed deep RNA-seq.
In particular, to identify physiologically relevant pathways promoting carcinogenesis in HOS, we compared HOS and healthy bone RNA-seq and performed differential gene expression (DEG) analyses among these two groups.
After normalisation, we analysed the principal component analysis (PCA) of all samples. The results showed that HOS samples and healthy bone samples separated from each other (Figure 16A). Then, we performed DEG analysis and obtained 1498 upregulated genes and 1198 downregulated genes (Figure 16B). The data were then adjusted according to the Monte Carlo simulation, obtaining 549 upregulated genes and 631 downregulated genes.
Considering the results after the Monte Carlo simulation, we found that in the HOS samples group, the G2M checkpoint, Epithelial Mesenchymal Transition (EMT), Mitotic Spindle and E2F-targets pathways were promoted, while Myogenesis, Fatty Acid Metabolism, Oxidative Phosphorylation, Adipogenesis and KRAS Signaling pathways were inhibited (Figure 17).

To gain insights into the transcriptional programmes of the metastatic and poor prognosis tumours, we collected gene expression data of metastatic patients compared to that of localised patients.
After normalisation, we analysed the PCA1 and 2 of all samples and the results showed that HOS samples derived from metastatic patients and HOS samples derived from localised patients separated from each other (Figure 18). By performing DEG analysis, we identified 337 up-regulated and 292 down-regulated genes (Supplementary Table 1) in patients with metastatic HOS compared to patients with a localised disease. We then evaluated the over-representation of these differentially expressed genes.
Metastatic disease was significantly characterised by the up-regulation of genes involved in the "Hallmark - Inflammatory Response Signature" compared to localised disease, thus corroborating the role of tumour inflammation in cancer dissemination (41)(42).

Among the genes involved in the inflammatory response pathway, we confirmed the presence of genes that have been recurrently described in HOS dissemination or the HOS chemo-resistance process, as summarised in Table 7 (43)(44)(45)(46)(47)(48). Interestingly, our analysis demonstrated the role of SCARF1, PTPRE, P2RY2, GNA15, FZD5, CCRL2, C5AR1 and AQP9 in the HOS cancer invasion and metastasis process and this finding, to our knowledge, has not been previously reported in literature.

Furthermore, in addition to the presence of a prominent inflammatory component, the DEG analysis showed that the metastasis process was characterised also by a concomitant upregulation of BCL2L1 and EPCAM.

It has been previously reported that the BCL2L1 is a key regulator of apoptosis, which promotes apoptosis evasion, autophagy, and metastasis in various cancer cells (49) and high BCL2L1 expression was identified in the primary HOS tumour correlating with metastasis at diagnosis and a worse Event-Free Survival (50). EPCAM, epithelial cell adhesion molecule, is a glycoprotein that mediates cell-cell adhesion and regulates cell proliferation and differentiation, and its overexpression has been associated with poor prognosis in a variety of cancers (51).

DISCUSSION

SARGEN projects demonstrated that the conduction of a prospective multi-centre translational research project for rare tumours, such as BS, is feasible and the infrastructure to offer genomic analysis to young patients with BS in Italy was established. Thanks to these projects, the comprehensive sequencing of HOS and EWS has become more widespread across the AIEOP Centres, with the aim of identifying clinically relevant alterations for a matched targeted therapy and to explore in depth the tumour molecular features and processes.

Although the processing of BS tissue could be more difficult than expected, due to the paucity of material from bone tissue biopsies and/or decalcification process, SARGEN projects reported a high WXS and RNA-Seq success rate. Nevertheless, a fresh or fresh-frozen sample would be preferable, especially for HOS samples.

Consistent with other international experiences (32)(33)(52)(34), about 58% of patients had one or more “potentially actionable” genomic tumour alterations. However, the number of patients who underwent a matched targeted therapy was lower than other experiences reported in the literature (15.7% of relapsed patients). This discrepancy is probably because our study is specifically dedicated to BS only. It is known that BS, especially HOS, do not have a known targeted driver alteration compared to other kind of paediatric tumours (e.g. low-grade glioma, anaplastic large cell lymphoma, inflammatory myofibroblastic tumour, etc..) and the benefit of targeted matched therapy is still under investigation in this context (53). Moreover, it is necessary to increase the new target drugs trial availability for paediatric patients across countries (21% of relapsed patients with a potential target did not receive any specific drug due to drug non-availability for children) and it will be important to anticipate the sequencing analyses at the very early relapse (26.5% of relapsed patients with a potential target did not receive matched treatment because of a rapid tumour progression).

Although, up to now, the number of patients who benefit from a new target treatment is still low, translational research projects such as SARGEN trials are crucial to identify the rare patients with a “potentially actionable” alteration, increasing drug discovery and enrolling them in new investigational clinical trials. Moreover, these projects are essential to accelerate the genomic

research in rare BS where the molecular mechanisms related to carcinogenesis, progression and resistance to therapy are still largely unknown.
In this thesis, a comprehensive genomic analysis of HOS samples is reported which confirms the heterogeneous and complex genomic landscape of this tumour. HOS samples are characterised by a low tumour mutational burden and a high chromosomal instability. There are specific unstable regions (Figure 13) that are more sensitive to structural variations and inside these we found important oncogenes or onco-suppressor genes altered in more than 80% of their structure. MYC is the most common amplified gene (73% of samples) and TP53 is the most common deleted gene (51%), highlighting their initiating role in HOS development (54)(55).
Indeed, a high MYC amplification correlates with a MYC gain-of-function (56)(57). MYC activation induces Double-Strands-Break (DSB), at least in part through the generation of oxidative stress, and compromised the p53-dependent cell cycle arrest response triggered by DNA damage promoting the entry of numerous cells into the cycle (41)(57). As previously described, our cohort showed a high incidence of p53-deletion. The presence of the inactivation of the p53-dependent apoptotic response and the increased genetic instability that accompany loss of the p53 pathway are highly selected during cancer progression (57). However, the presence of p53 deficiency alone is insufficient for induction of genetic instability. Consistent with this concept, the co-presence of MYC amplification and TP53 deletion in our samples explain their synergic role in HOS tumorigenesis: their combined effect increases the genome destabilisation and accelerates multi-stage tumour progression in HOS biology.
Interesting results emerged by comparing the RNA-seq data of HOS samples derived from metastatic and localised patients. Metastatic disease was significantly characterised by the up-regulation of genes involved in the “Hallmark - Inflammatory Response Signature” compared to localised disease. In particular, thirteen genes involved in this signature were significantly upregulated in metastatic tumour correlating with a worse patient prognosis. Five of them were already known in HOS biology (Table 7), while SCARF1, PTPRE, P2RY2, GNA15, FZD5, CCRL2, C5AR1 and AQP9 are newcomers in HOS. Our data corroborate that tumour-associated inflammatory response enhances tumorigenesis and progression (41)(42). Inflammation contributes to multiple hallmark capabilities by supplying mediator factors to the tumour microenvironment, including factors that sustain proliferative signalling, limit cell death, facilitate angiogenesis, invasion, and metastasis, and inductive signals that lead to activation of EMT and other hallmark-facilitating programs (42). Furthermore, cancer-related inflammation contributes to the genetic instability of cancer cells (41) which is a peculiarity of HOS.
Interestingly, our data suggest a synergic role of BCL2L1 and EPCAM up-regulation in the cancer dissemination. Indeed, in addition to the up-regulation of the “Hallmark - Inflammatory Response Signature”, samples derived from metastatic patients showed a statistically significant over-expression of BCL2L1 and EPCAM. BCL2L1 acts as an apoptotic inhibitor. It has been previously reported that a tumour-related inflammatory context promotes survival in tumour cells, by inducing antiapoptotic genes (41) such as BCL2L1 of our metastatic cohort. EPCAM is implicated in invasion and metastasis process (51).

The genomic results of the whole HOS cohort support our hypothesis of the metastasis process in HOS. The aggressive behaviour of metastatic HOS is explained by the combined effect of MYC and TP53 in addition to an up-regulated Cancer Immune Response Pathway. Indeed, it is known that

inflammatory mediators induce DSB in cancer cells (41). Usually there are two major mechanisms to repair DSB: homologous recombination (HR) and non-homologous end joining (41)(57)(58). The genome integrity is impaired by the increase of DSB, and precise regulation of the error-free HR mechanisms is essential for genome stability since uncontrolled HR excess promotes tumour inflammation as well as HR deficiency (41). More than one third of HOS samples are enriched with CN17 signature, which describes a HR deficiency tumour. This feature increases the tumour genome destabilisation, fostering the proliferation process in cancer characterised by a combined presence of MYC amplification, TP53 inactivation, anti-apoptotic effect induced by BCL2L1 overexpression and EPCAM upregulation.

REFERENCES

1. Choi EYK, Gardner JM, Lucas DR, McHugh JB, Patel RM. Ewing sarcoma. Seminars in Diagnostic Pathology. 2014 Jan;31(1):39–47.
2. Gianferante DM, Mirabello L, Savage SA. Germline and somatic genetics of osteosarcoma — connecting aetiology, biology and therapy. Nat Rev Endocrinol. 2017 Aug;13(8):480–91.
3. Tirtei E, Asaftei SD, Manicone R, Cesari M, Paioli A, Rocca M, et al. Survival after second and subsequent recurrences in osteosarcoma: a retrospective multicenter analysis. Tumori. 2018 Jun;104(3):202–6.
4. Tirtei E, Cereda M, De Luna E, Quarello P, Asaftei SD, Fagioli F. Omic approaches to pediatric bone sarcomas. Pediatric Blood & Cancer. 2020 Feb;67(2):e28072.
5. Shi S, Wang Q, Du X. Comprehensive bioinformatics analysis reveals the oncogenic role of FoxM1 and its impact on prognosis, immune microenvironment, and drug sensitivity in osteosarcoma. J Appl Genetics. 2023 Dec;64(4):779–96.
6. Hasin Y, Seldin M, Lusis A. Multi-omics approaches to disease. Genome Biol. 2017 Dec;18(1):83.
7. Cereda M, Gambardella G, Benedetti L, Iannelli F, Patel D, Basso G, et al. Patients with genetically heterogeneous synchronous colorectal cancer carry rare damaging germline mutations in immune-related genes. Nat Commun. 2016 Jul 5;7(1):12072.
8. Morandi E, Cereda M, Incarnato D, Parlato C, Basile G, Anselmi F, et al. HaTSPiL: A modular pipeline for high-throughput sequencing data analysis. Kalendar R, editor. PLoS ONE. 2019 Oct 15;14(10):e0222512.
9. Broad Institute. Picard Tools. https://broadinstitute.github.io/picard/ (2022).
10. Cibulskis K, Lawrence MS, Carter SL, Sivachenko A, Jaffe D, Sougnez C, et al. Sensitive detection of somatic point mutations in impure and heterogeneous cancer samples. Nat Biotechnol. 2013 Mar;31(3):213–9.
11. Saunders CT, Wong WSW, Swamy S, Becq J, Murray LJ, Cheetham RK. Strelka: accurate somatic small-variant calling from sequenced tumor–normal sample pairs. Bioinformatics. 2012 Jul 15;28(14):1811–7.
12. Koboldt DC, Zhang Q, Larson DE, Shen D, McLellan MD, Lin L, et al. VarScan 2: Somatic mutation and copy number alteration discovery in cancer by exome sequencing. Genome Res. 2012 Mar;22(3):568–76.
13. Li Q, Wang K. InterVar: Clinical Interpretation of Genetic Variants by the 2015 ACMG-AMP Guidelines. The American Journal of Human Genetics. 2017 Feb;100(2):267–80.
14. Richards S, Aziz N, Bale S, Bick D, Das S, Gastier-Foster J, et al. Standards and guidelines for the interpretation of sequence variants: a joint consensus recommendation of the American College of Medical Genetics and Genomics and the Association for Molecular Pathology. Genetics in Medicine. 2015 May;17(5):405–24.
15. Berrino E, Filippi R, Visintin C, Peirone S, Fenocchio E, Farinea G, et al. Collision of germline POLE and PMS2 variants in a young patient treated with immune checkpoint inhibitors. npj Precis Onc. 2022 Mar 8;6(1):15.

16. Favero F, Joshi T, Marquard AM, Birkbak NJ, Krzystanek M, Li Q, et al. Sequenza: allele-specific copy number and mutation profiles from tumor sequencing data. Annals of Oncology. 2015 Jan;26(1):64–70.
17. Mermel CH, Schumacher SE, Hill B, Meyerson ML, Beroukhim R, Getz G. GISTIC2.0 facilitates sensitive and confident localization of the targets of focal somatic copy-number alteration in human cancers. Genome Biol. 2011 Apr;12(4): R41.
18. An O, Dall'Olio GM, Mourikis TP, Ciccarelli FD. NCG 5.0: updates of a manually curated repository of cancer genes and associated properties from cancer mutational screenings. Nucleic Acids Res. 2016 Jan 4;44(D1):D992–9.
19. Wang K, Li M, Hakonarson H. ANNOVAR: functional annotation of genetic variants from high-throughput sequencing data. Nucleic Acids Research. 2010 Sep 1;38(16): e164–e164.
20. Melloni GEM, Guida A, Curigliano G, Botteri E, Esposito A, Kamal M, et al. Precision Trial Drawer, a Computational Tool to Assist Planning of Genomics-Driven Trials in Oncology. JCO Precision Oncology. 2018 Nov;(2):1–16.
21. Li MM, Datto M, Duncavage EJ, Kulkarni S, Lindeman NI, Roy S, et al. Standards and Guidelines for the Interpretation and Reporting of Sequence Variants in Cancer. The Journal of Molecular Diagnostics. 2017 Jan;19(1):4–23.
22. Islam SMA, Díaz-Gay M, Wu Y, Barnes M, Vangara R, Bergstrom EN, et al. Uncovering novel mutational signatures by de novo extraction with SigProfilerExtractor. Cell Genomics. 2022 Nov;2(11):100179.
23. Steele CD, Abbasi A, Islam SMA, Bowes AL, Khandekar A, Haase K, et al. Signatures of copy number alterations in human cancer. Nature. 2022 Jun 30;606(7916):984–91.
24. Wang S, Li H, Song M, Tao Z, Wu T, He Z, et al. Copy number signature analysis tool and its application in prostate cancer reveals distinct mutational processes and clinical outcomes. Gordenin DA, editor. PLoS Genet. 2021 May 4;17(5): e1009557.
25. Wang S, Tao Z, Wu T, Liu XS. Sigflow: an automated and comprehensive pipeline for cancer genome mutational signature analysis. Pier Luigi M, editor. Bioinformatics. 2021 Jul 12;37(11):1590–2.
26. Bushnell, B. BBMap: A Fast, Accurate, Splice-Aware Aligner. https://www.osti.gov/servlets/purl/1241166 (2014).
27. Frankish A, Diekhans M, Ferreira AM, Johnson R, Jungreis I, Loveland J, et al. GENCODE reference annotation for the human and mouse genomes. Nucleic Acids Research. 2019 Jan 8;47(D1):D766–73.
28. Del Giudice M, Foster JG, Peirone S, Rissone A, Caizzi L, Gaudino F, et al. FOXA1 regulates alternative splicing in prostate cancer. Cell Reports. 2022 Sep;40(13):111404.
29. Wu T, Hu E, Xu S, Chen M, Guo P, Dai Z, et al. clusterProfiler 4.0: A universal enrichment tool for interpreting omics data. The Innovation. 2021 Aug;2(3):100141.
30. Yu G, Wang LG, Han Y, He QY. clusterProfiler: an R Package for Comparing Biological Themes Among Gene Clusters. OMICS: A Journal of Integrative Biology. 2012 May;16(5):284–7.
31. Subramanian A, Tamayo P, Mootha VK, Mukherjee S, Ebert BL, Gillette MA, et al. Gene set enrichment analysis: A knowledge-based approach for interpreting genome-wide expression profiles. Proc Natl Acad Sci USA. 2005 Oct 25;102(43):15545–50.
32. Berlanga P, Pierron G, Lacroix L, Chicard M, Adam De Beaumais T, Marchais A, et al. The European MAPPYACTS Trial: Precision Medicine Program in Pediatric and Adolescent Patients with Recurrent Malignancies. Cancer Discovery. 2022 May 2;12(5):1266–81.
33. Church AJ, Corson LB, Kao PC, Imamovic-Tuco A, Reidy D, Doan D, et al. Molecular profiling identifies targeted therapy opportunities in pediatric solid cancer. Nat Med. 2022 Aug;28(8):1581–9.
34. Worst BC, Van Tilburg CM, Balasubramanian GP, Fiesel P, Witt R, Freitag A, et al. Next-generation personalised medicine for high-risk paediatric cancer patients – The INFORM pilot study. European Journal of Cancer. 2016 Sep; 65:91–101.
35. Sosinsky A, Ambrose J, Cross W, Turnbull C, Henderson S, Jones L, et al. Insights for precision oncology from the integration of genomic and clinical data of 13,880 tumors from the 100,000 Genomes Cancer

Programme. Nat Med [Internet]. 2024 Jan 11 [cited 2024 Jan 20]; Available from: https://www.nature.com/articles/s41591-023-02682-0
36. Mateo J, Chakravarty D, Dienstmann R, Jezdic S, Gonzalez-Perez A, Lopez-Bigas N, et al. A framework to rank genomic alterations as targets for cancer precision medicine: the ESMO Scale for Clinical Actionability of molecular Targets (ESCAT). Annals of Oncology. 2018 Sep;29(9):1895–902.
37. Thatikonda V, Islam SMA, Autry RJ, Jones BC, Gröbner SN, Warsow G, et al. Comprehensive analysis of mutational signatures reveals distinct patterns and molecular processes across 27 pediatric cancers. Nat Cancer. 2023 Jan 26;4(2):276–89.
38. ICGC PedBrain-Seq Project, ICGC MMML-Seq Project, Gröbner SN, Worst BC, Weischenfeldt J, Buchhalter I, et al. The landscape of genomic alterations across childhood cancers. Nature. 2018 Mar 15;555(7696):321–7.
39. Yang L, Roberts D, Takhar M, Erho N, Bibby BAS, Thiruthaneeswaran N, et al. Development and Validation of a 28-gene Hypoxia-related Prognostic Signature for Localized Prostate Cancer. EBioMedicine. 2018 May;31:182–9.
40. Hadi K, Yao X, Behr JM, Deshpande A, Xanthopoulakis C, Tian H, et al. Distinct Classes of Complex Structural Variation Uncovered across Thousands of Cancer Genome Graphs. Cell. 2020 Oct 1;183(1):197-210.e32.
41. Colotta F, Allavena P, Sica A, Garlanda C, Mantovani A. Cancer-related inflammation, the seventh hallmark of cancer: links to genetic instability. Carcinogenesis. 2009 Jul 1;30(7):1073–81.
42. Hanahan D, Weinberg RA. Hallmarks of Cancer: The Next Generation. Cell. 2011 Mar;144(5):646–74.
43. Li Q, Chen G, Jiang H, Dai H, Li D, Zhu K, et al. ITGB3 promotes cisplatin resistance in osteosarcoma tumors. Cancer Med. 2023 Apr;12(7):8452–63.
44. Jiang L, Jiang S, Zhou W, Huang J, Lin Y, Long H, et al. Oxidized low density lipoprotein receptor 1 promotes lung metastases of osteosarcomas through regulating the epithelial-mesenchymal transition. J Transl Med. 2019 Dec;17(1):369.
45. Morrow JJ, Bayles I, Funnell APW, Miller TE, Saiakhova A, Lizardo MM, et al. Positively selected enhancer elements endow osteosarcoma cells with metastatic competence. Nat Med. 2018 Feb 1;24(2):176–85.
46. Shi Z, Zhou H, Pan B, Lu L, Wei Z, Shi L, et al. Exploring the key genes and pathways of osteosarcoma with pulmonary metastasis using a gene expression microarray. Molecular Medicine Reports. 2017 May;16(5):7423–31.
47. Avnet S, Lemma S, Cortini M, Di Pompo G, Perut F, Lipreri MV, et al. The Release of Inflammatory Mediators from Acid-Stimulated Mesenchymal Stromal Cells Favours Tumour Invasiveness and Metastasis in Osteosarcoma. Cancers. 2021 Nov 22;13(22):5855.
48. Wen ZQ, Li XG, Zhang YJ, Ling ZH, Lin XJ. Osteosarcoma cell-intrinsic colony stimulating factor-1 receptor functions to promote tumor cell metastasis through JAG1 signaling. Am J Cancer Res. 2017;7(4):801–15.
49. Li M, Wang D, He J, Chen L, Li H. Bcl-XL: A multifunctional anti-apoptotic protein. Pharmacological Research. 2020 Jan;151:104547.
50. Trujillo-Paolillo A, Tesser-Gamba F, Seixas Alves M, Filho R, Oliveira R, Petrilli A, et al. Pharmacogenetics of the Primary and Metastatic Osteosarcoma: Gene Expression Profile Associated with Outcome. IJMS. 2023 Mar 15;24(6):5607.
51. Schnell U, Cirulli V, Giepmans BNG. EpCAM: Structure and function in health and disease. Biochimica et Biophysica Acta (BBA) - Biomembranes. 2013 Aug;1828(8):1989–2001.
52. Harris MH, DuBois SG, Glade Bender JL, Kim A, Crompton BD, Parker E, et al. Multicenter Feasibility Study of Tumor Molecular Profiling to Inform Therapeutic Decisions in Advanced Pediatric Solid Tumors: The Individualized Cancer Therapy (iCat) Study. JAMA Oncol. 2016 May 1;2(5):608.
53. Tirtei E, Campello A, Asaftei SD, Mareschi K, Cereda M, Fagioli F. Precision Medicine in Osteosarcoma: MATCH Trial and Beyond. Cells. 2021 Jan 31;10(2):281.

54. Marinoff AE, Spurr LF, Fong C, Li YY, Forrest SJ, Ward A, et al. Clinical Targeted Next-Generation Panel Sequencing Reveals MYC Amplification Is a Poor Prognostic Factor in Osteosarcoma. JCO Precision Oncology. 2023 Mar;(7): e2200334.
55. Bousquet M, Noirot C, Accadbled F, Sales De Gauzy J, Castex MP, Brousset P, et al. Whole-exome sequencing in osteosarcoma reveals important heterogeneity of genetic alterations. Annals of Oncology. 2016 Apr;27(4):738–44.
56. https://www.oncokb.org.
57. Vafa O, Wade M, Kern S, Beeche M, Pandita TK, Hampton GM, et al. c-Myc Can Induce DNA Damage, Increase Reactive Oxygen Species, and Mitigate p53 Function. Molecular Cell. 2002 May;9(5):1031–44.
58. Stewart MD, Merino Vega D, Arend RC, Baden JF, Barbash O, Beaubier N, et al. Homologous Recombination Deficiency: Concepts, Definitions, and Assays. The Oncologist. 2022 Mar 11;27(3):167–74.

FIGURES AND TABLES

Figure 1. Study-flow.

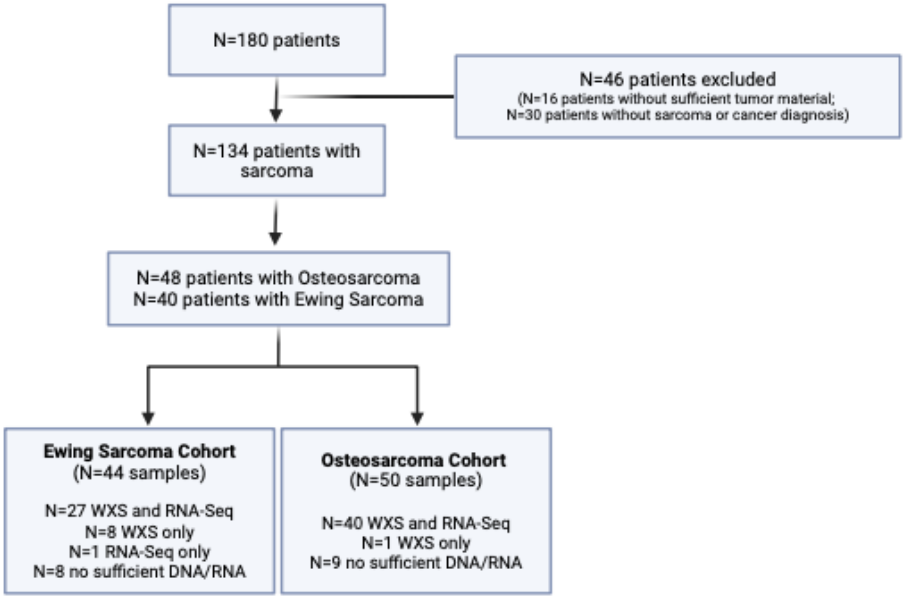

Figure 2. Patient's enrollment according to diagnosis

Disease	n° patients
Osteosarcoma	48
Ewing's Sarcoma	40
Rhabdomyosarcoma	14
Synovial Sarcoma	7
Alveolar Soft Tissue Sarcoma	4
Liposarcoma	4
Chondrosarcoma	3
Leiomyosarcoma	3
Others*	10

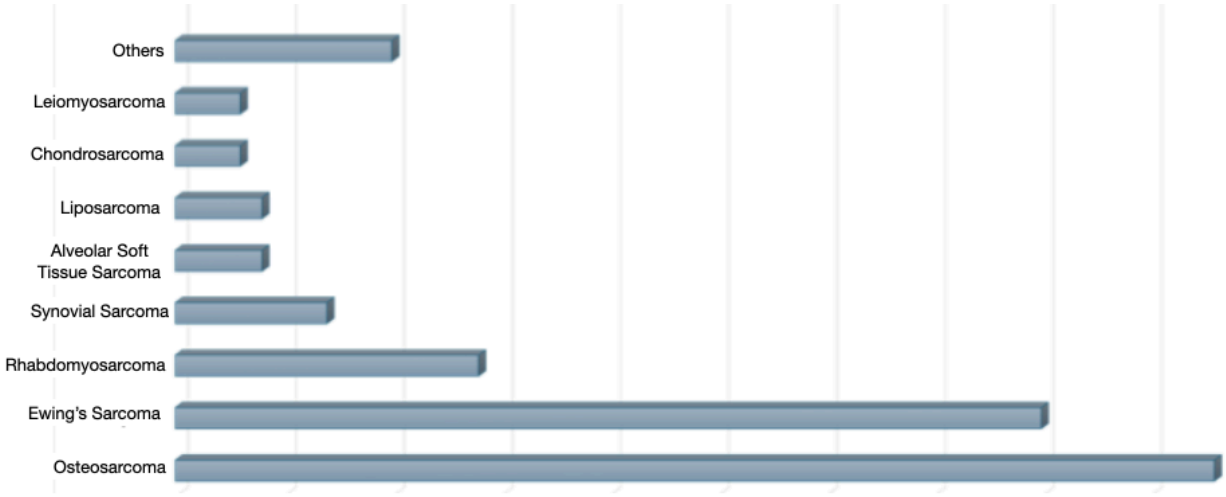

* Others: 1 Angiosarcoma, 1 Epitheliod Sarcoma, 1 Emangiothelioma, 1 Bone Malignant Istyocitoma, 1 Mesenchymal Tumor, 1 Malignant Peripheral Nerve Sheath Tumor, 1 Primitive Mesenchymal Tumor, 1 Infantile Fibrosarcoma, 2 Undifferentaited Sarcomas

Figure 3. Overall Survival

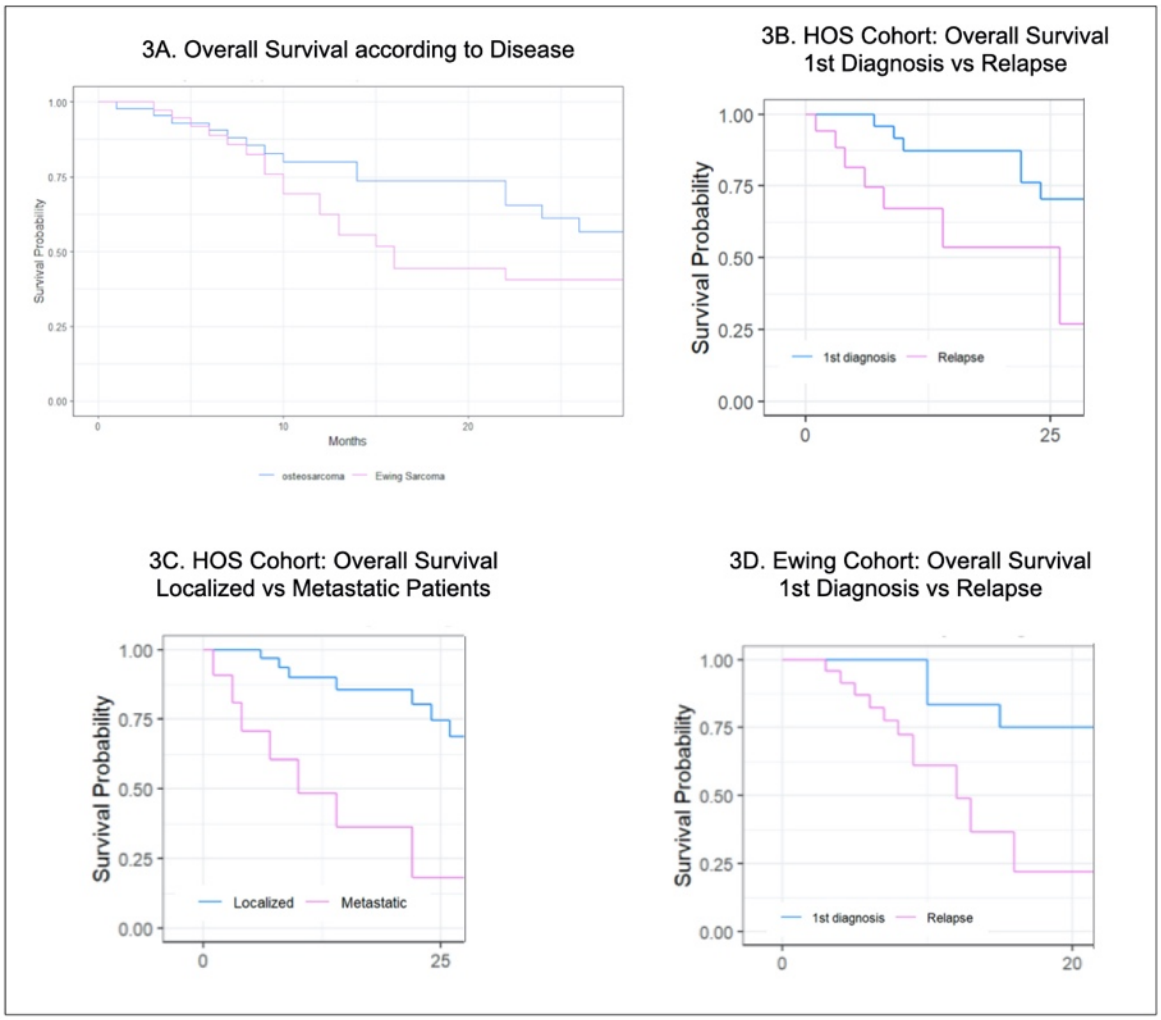

Table 1. Clinical characteristics of HOS patients

		N° HOS patients (tot. 48)	%
Sex	Male	25	52
	Female	23	48
Stadiation at enrollemnt	Localized	29	62
	Metastatic	17	36
	Unknown	1	2
Further Relapse	Yes	19	60
	No	29	40
Status at last FUP	Dead	19	40
	Alive	29	60

Table 2. HOS Sample characteristics

		N° of Samples with WXS +/- RNA-Seq (tot:41)	%
Sample procedure, site and timing	Resection - Mts at 1st diagnosis	2	5
	Biopsy - Mts at relapse	3	7
	Resection - Mts at relapse	1	2,5
	Biopsy - Primary Tumor at 1st Diagnosis	31	76
	Resection - Primary Tumor at 1st Diagnosis	1	2,5
	Biopsy - Primary Tumor at Relapse	2	4,5
	Resection - Primary Tumor at Relapse	1	2,5
Timing	1st Diagnosis	34	83
	Relapse	7	17
Histotype	Osteoblastic	22	53
	Chondroblastic	4	10
	Teleangiectatic	4	10
	Mixed Osteo/Chondroblastic	2	5
	Fibroblastic	2	5
	Not Specified	7	17
Organ	Bone	33	80
	Lung	5	12,5
	Soft Tissue	2	5
	Unknown	1	2,5
Sample Site	Femur	19	46
	Tibia	7	17
	Lung	5	12
	Hip	3	7,5
	Rib	2	5
	Diafragm	1	2,5
	Perone	1	2,5
	Sacrum	1	2,5
	Unknown	2	5

Table 3. EWS patient characteristics

		N° EWS patients (tot. 40)	%
Sex	Male	26	65
	Female	14	35
Stadiation at enrollemnt	Localized	14	35
	Metastatic	24	60
	Unknown	2	5
Further Relapse	Yes	21	52,5
	No	19	47,5
Status at last FUP	Dead	22	55
	Alive	18	45

Table 4. EWS sample characteristics

		N° of Samples with WXS +/- RNA-Seq (tot:36)	%
Sample procedure, site and timing:	Biopsy - Mts at relapse	12	33,3
	Resection - Mts at relapse	2	5,5
	Biopsy - Primary Tumor at 1st Diagnosis	13	36
	Biopsy - Primary Tumor at Relapse	7	19,5
	Resection - Primary Tumor at Relapse	2	5,5
Timing:	1st Diagnosis	13	36
	Relapse	23	64
Organ:	Bone	19	52,8
	Lung/Pleura	4	11
	Soft Tissue	11	30,5
	Brain	1	2,7
	Skin	1	2,7
Sample Site:	Femur	7	19,5
	Brain	1	2,7
	Lung/Pleura	3	8,3
	Hip	6	16,6
	Clavicle	1	2,7
	Mediastinum	2	5,5
	Omero	3	8,3
	Perone	1	2,7
	Scapola	5	13,8
	Skin	1	2,7
	Skull	1	2,7
	Ulna	1	2,7
	Vertebrae	4	11

Figure 4. List of the "potentially actionable" genomic findings in HOS Cohort

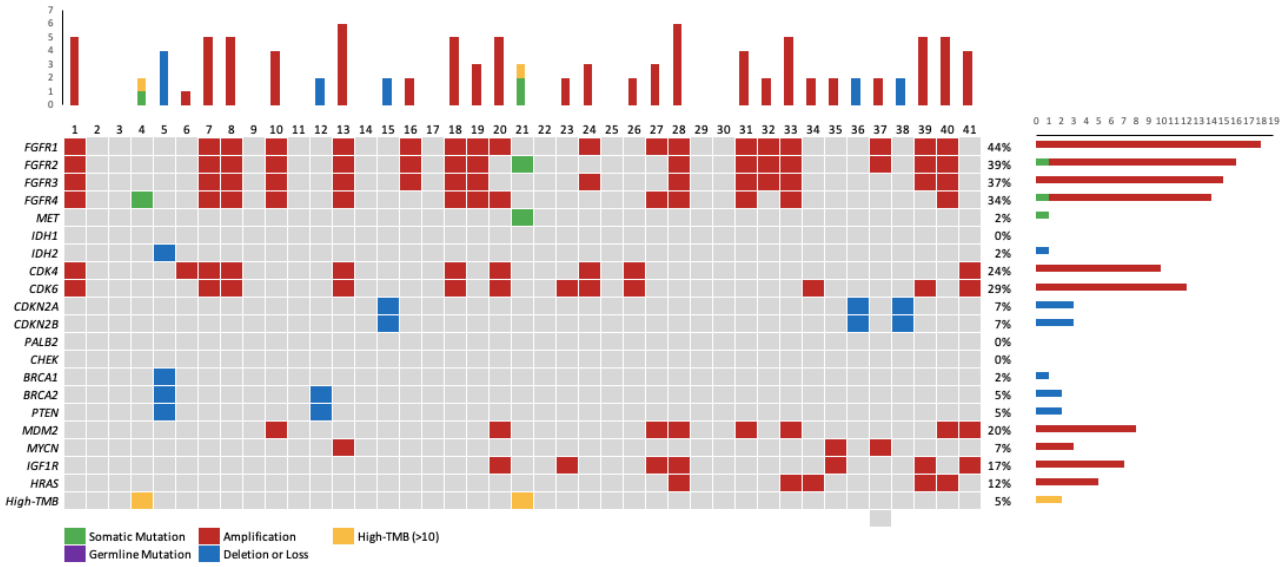

Figure 5. List of the "potentially actionable" genomic findings in EWS Cohort

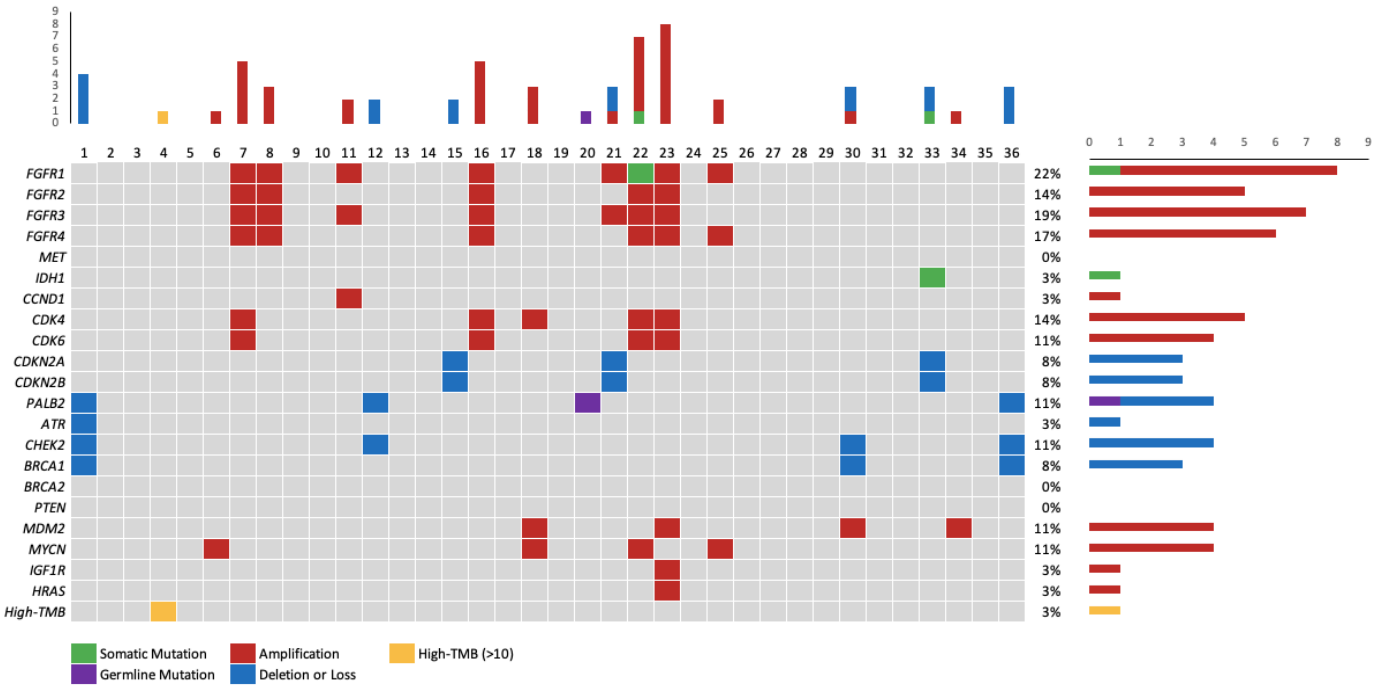

Table 5.

Patients treated with a matched therapy	**Total: 3/45 patients (6,5%) - 3/19 relapsed patients (15,7%)**	**Treatment type and follow-up**
	1 EWS pt with CCND1 amplification	PARP inhibitor + ATM/ATR inhibitor ongoing
	1 EWS pt with High-TMB	Immunotherapy – PD and exitus after an initial clinical benefit
	1 EWS pt with a pathogenic germline PALB2 mutation	Talazoparib + Temozolomide – PD and exitus after an initial clinical benefit
Patients not-treated with a matched therapy	**42/45 patients (93,3%)**	**Reason of no treatment**
	26 pts enrolled at first diagnosis (7 EWS + 19 HOS)	No further treatment needed
	4 pts: 2nd chemo ongoing	No further treatment needed
	3 pts: 2nd Complete Remission achieved	No further treatment needed
	5 pts with rapid PD	No clinical conditions for further treatment
	4 pts without drugs available	No specific trial open at that time or no off-label or compassionate drug use available

Figure 6. Nucleotide substitutions distribution across HOS samples

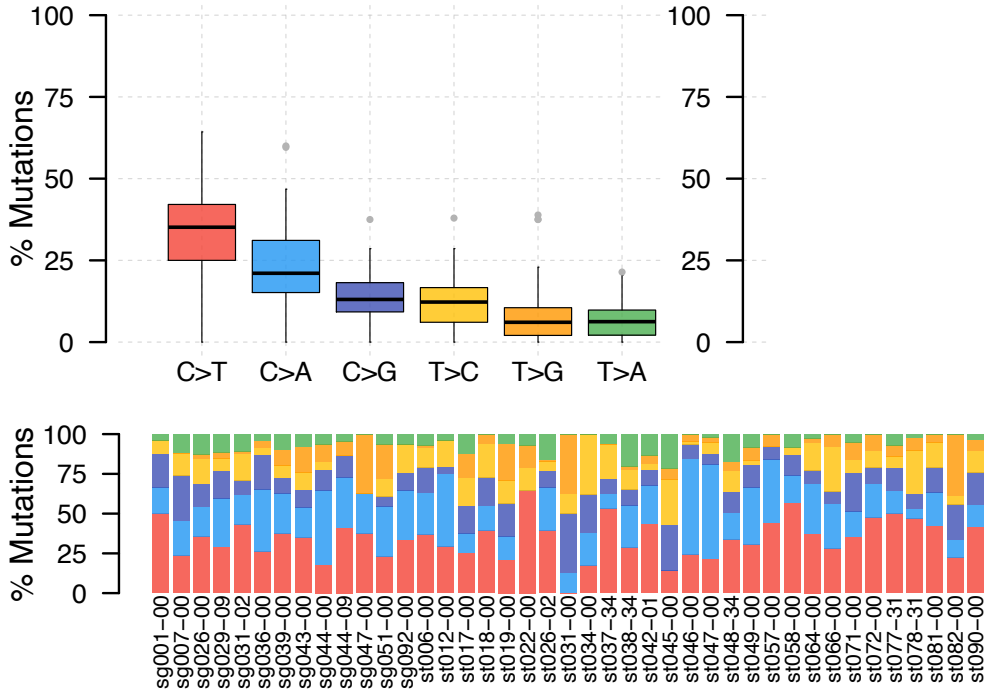

Figure 7. SBS signatures across HOS samples

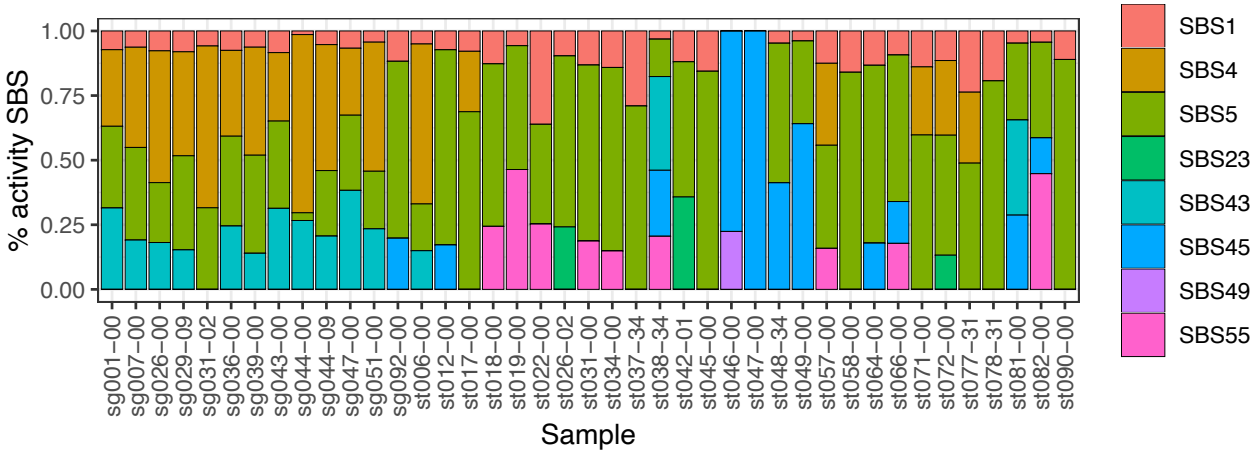

Figure 8. Extraction of a de novo signature which is a mixture of SBS5, SBS1 and SBS23

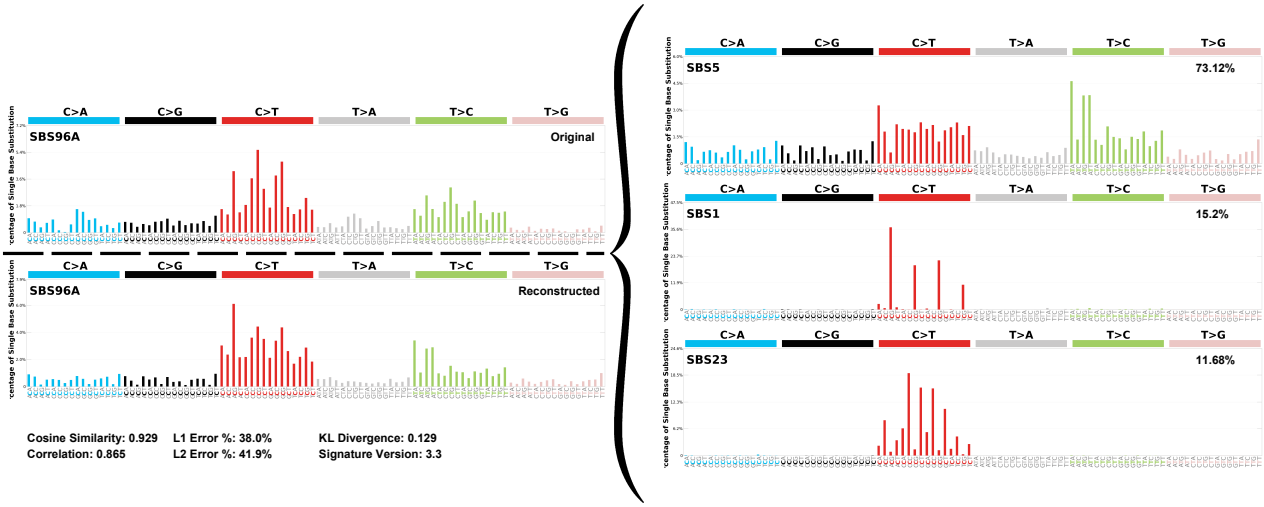

Figure 9. ID signatures across HOS samples

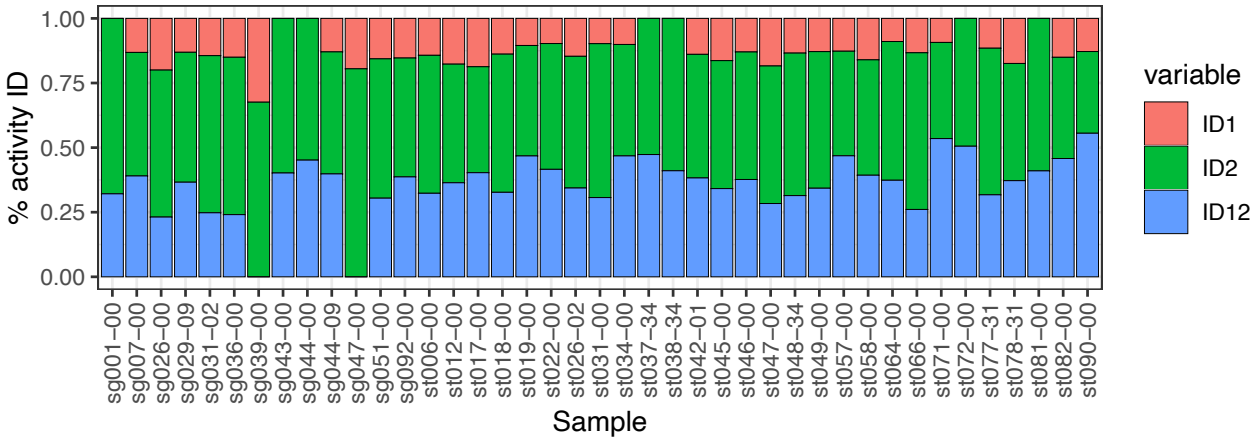

Figure 10. Extraction of a de novo signature which is a mixture of ID2, ID12 and ID1

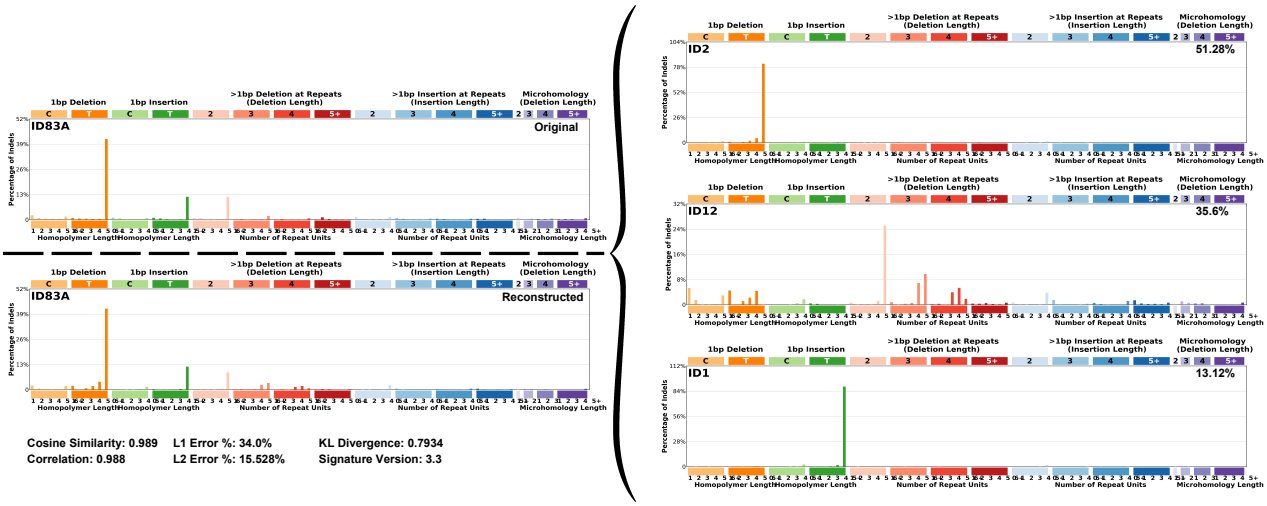

Figure 11.

A) Tumor Mutational Burden – HOS Cohort. Median value: 0,61 muts/Mb (range: 0,17-2,49).
B) Copy Number Alteration Burden – HOS Cohort. Median value: 95% (range: 1,2%-100%).

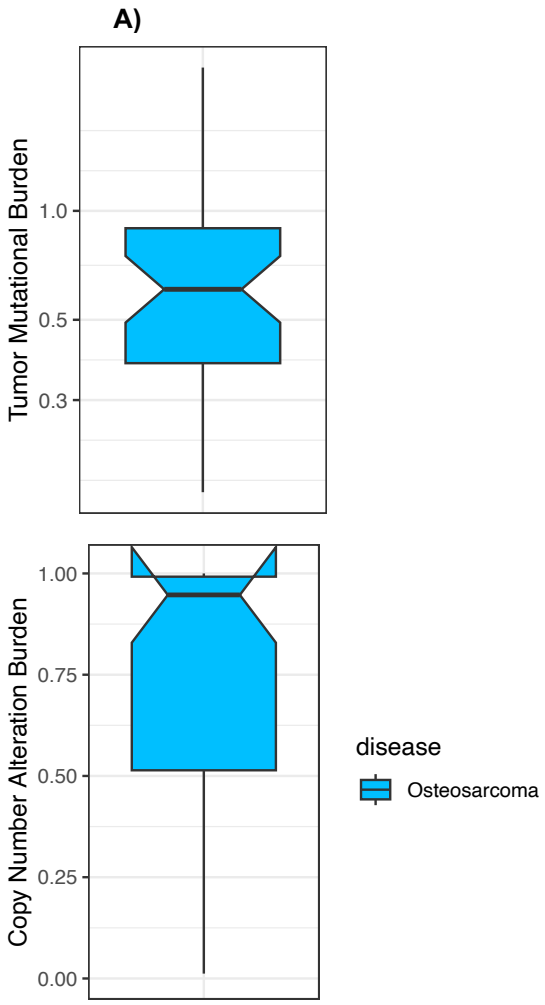

Figure 12. Most commonly mutated genes in HOS cohort.

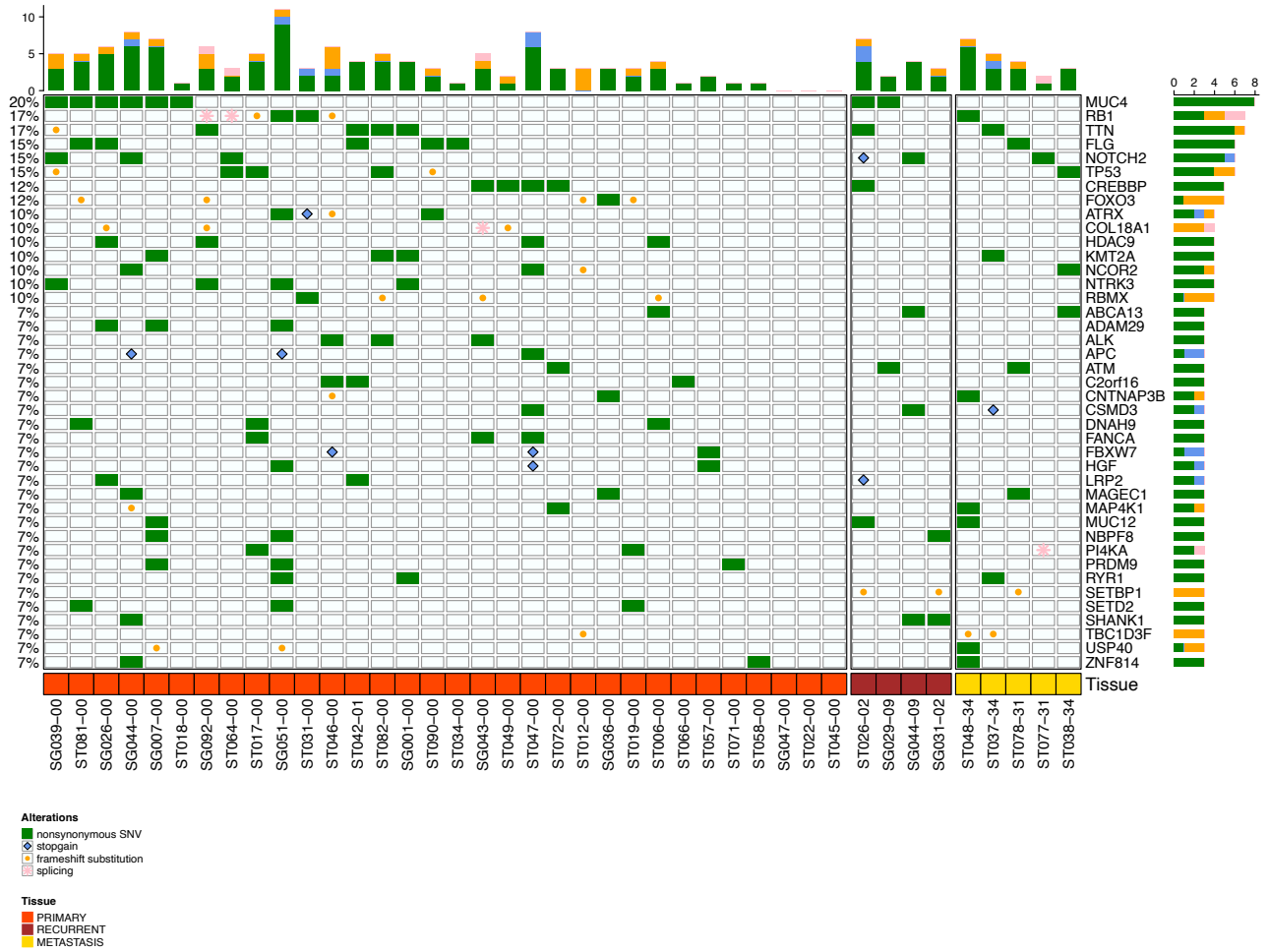

Figure 13. Most commonly amplified and deleted cytobands/regions – HOS Cohort.

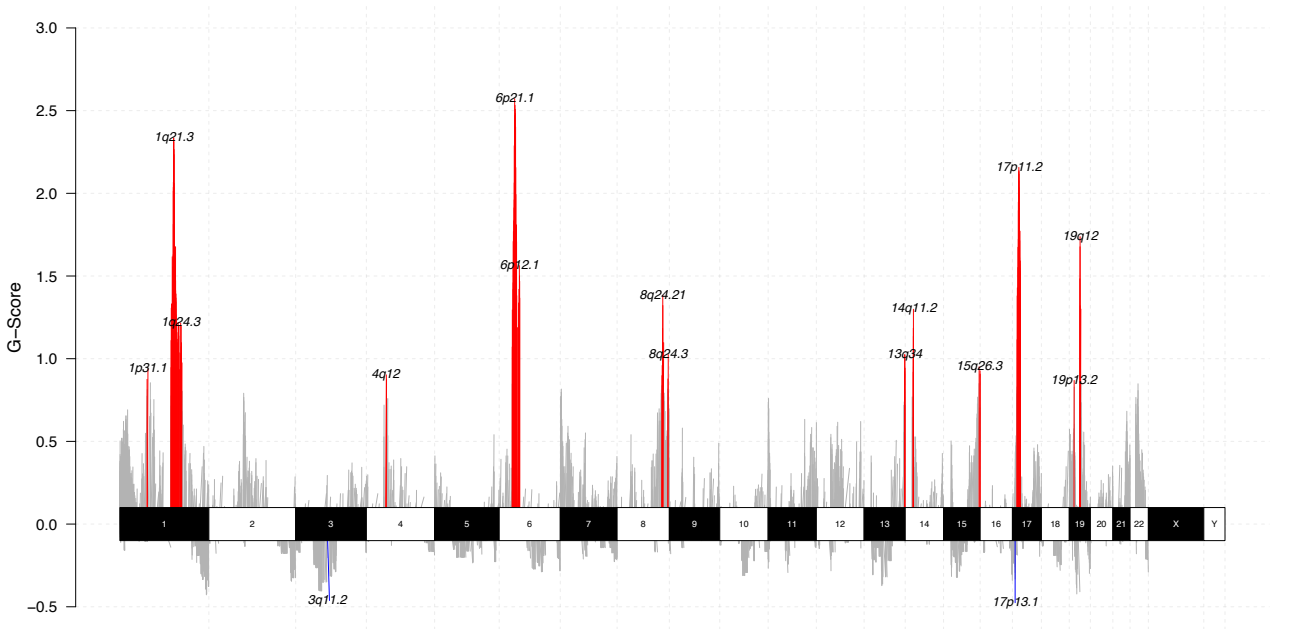

Table 6. List of most commonly amplified and deleted genes – HOS Cohort.

Gene	Variant Classification	% of samples
MYC	Amp	73%
ARNT	Amp	68%
MLLT11	Amp	68%
BCL10	Amp	63,5%
FUBP1	Amp	63,5%
RPL5	Amp	63,5%
HSP90AB1	Amp	58,5%
PRRX1	Amp	53,5%
TP53	Del	51%
CCNE1	Amp	44%
CHIC2	Amp	44%
FIP1L1	Amp	44%
KDR	Amp	44%
KIT	Amp	44%
PDGFRA	Amp	44%
CBLB	Del	29%
TFG	Del	29%
LYL1	Amp	27%
Amp=Amplification; Del=Deletion		

Figure 14. CN signatures across HOS samples

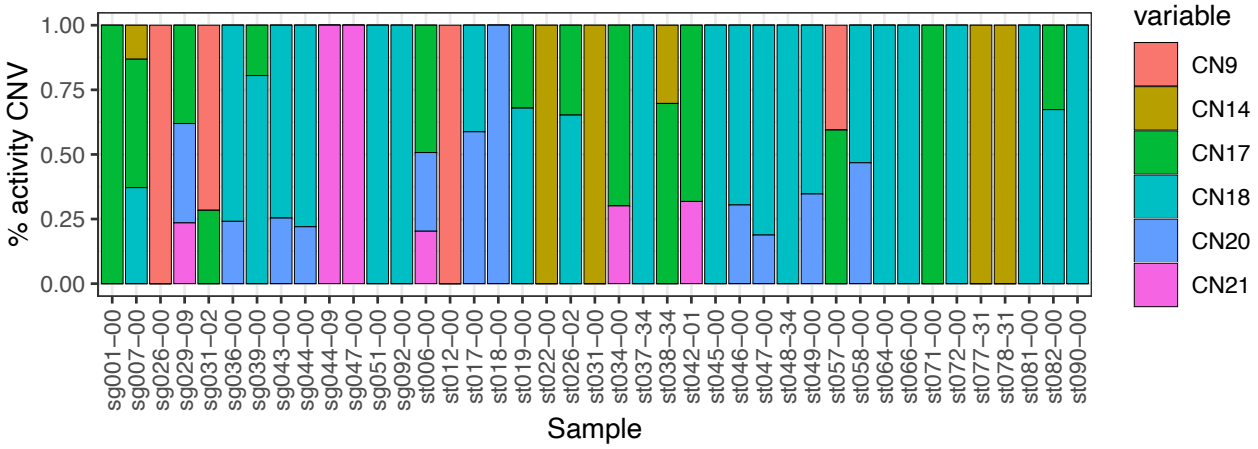

Figure 15. Extraction of a de novo signature which is a mixture of CN18 and CN20

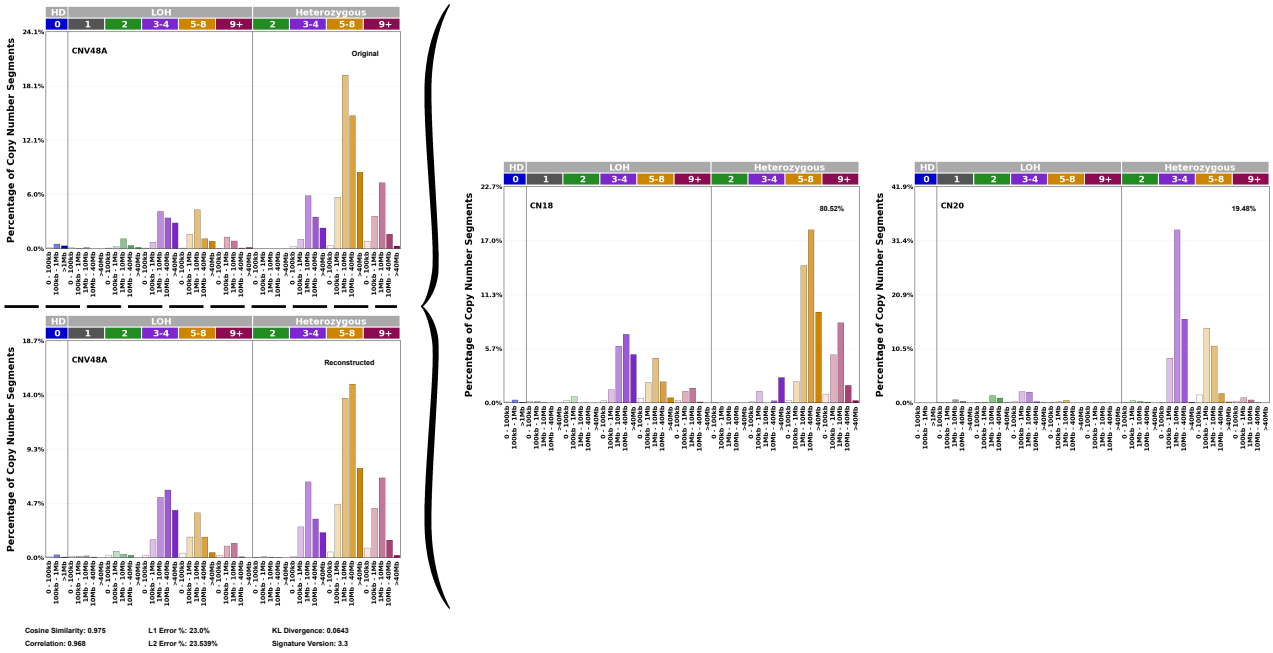

Figure 16. DEGs between HOS samples and Healthy Bone Samples.

A) Samples distribution was demonstrated by PCA.
B) DEGs were screened at the threshold of |log2FC|> =1 and adj.P.Val < 0.001

A)

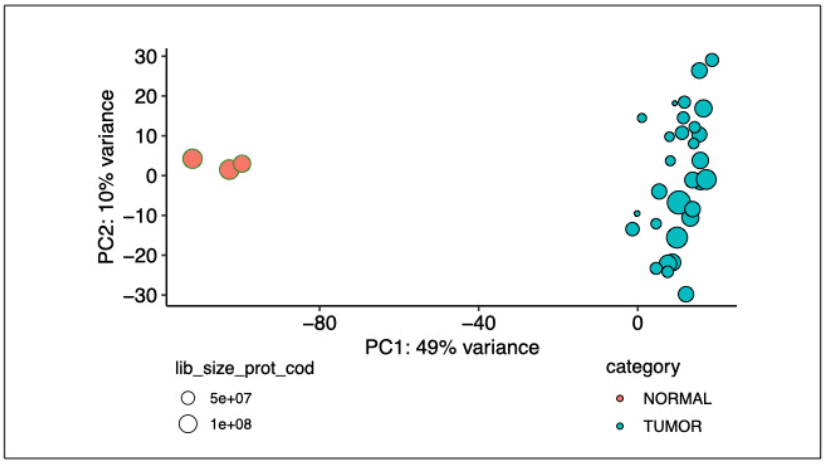

B)

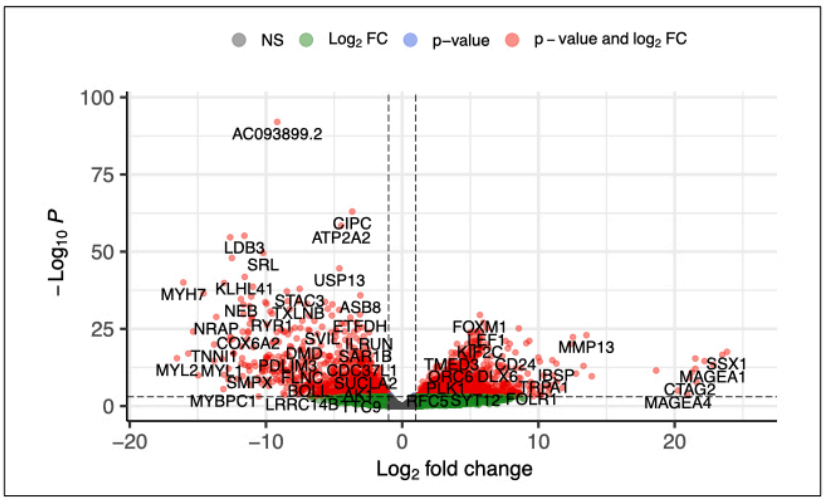

Figure 17: List of upregulated and downregulated pathways in HOS samples compared to Healthy Bone Samples

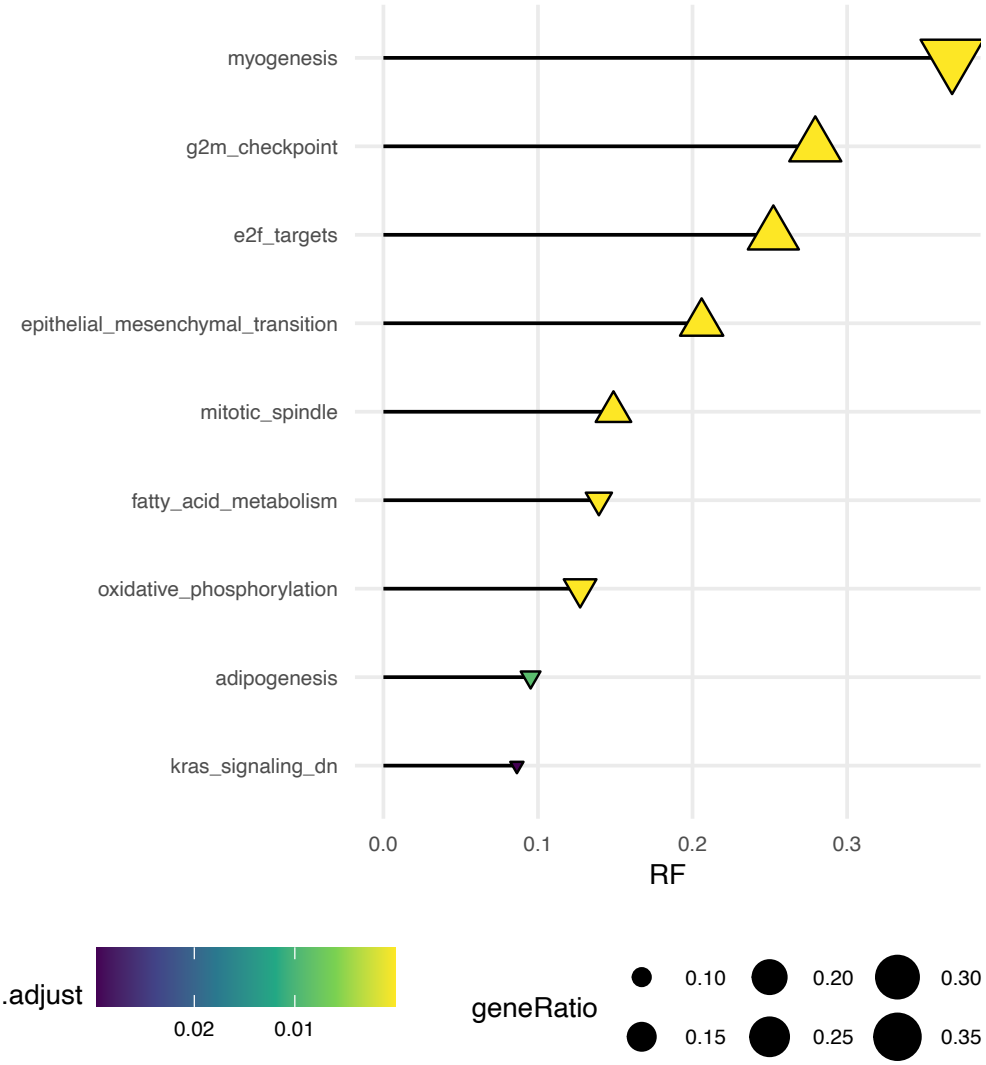

Figure 18. Samples distribution (samples derived from patients with metastatic HOS vs samples derived from patients with localized HOS) was demonstrated by PCA.

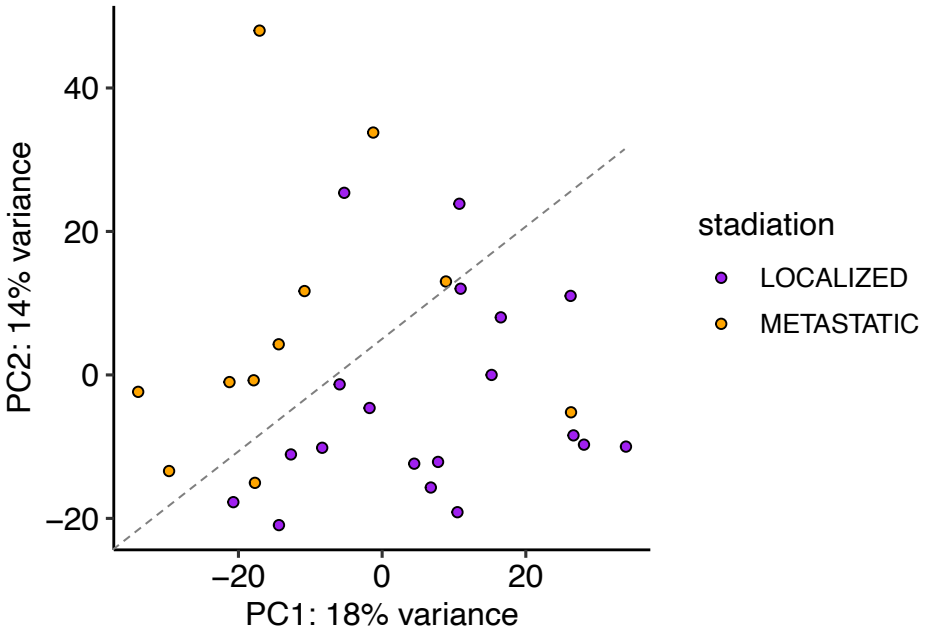

Table 7. Genes involved in the "Inflammatory Response Hallmark Pathway" already described in HOS

Gene	Known function in HOS samples	References
OLR1	OLR1 regulates EMT and thus promotes lung metastasis in HOS.	Jiang L. et al. 2019
ITGB3	ITGB3 was identified as a regulator of tumorigenicity and cisplatin resistance in relapsed HOS. Furthermore, the decreased HOS cell proliferation and migration ability in ITGB3 knockout HOS cells were related to increased apoptosis and slowing cell cycle progression.	Li Q. et al. 2023
IL6	Recent analyses of HOS transcriptome have highlighted IL6 as one of the risk factors most frequently associated with the onset of metastasis.	Avnet S. et al., 2021 – Shi Z. et al. 2017
F3	F3 emerged as a top candidate driver of metastasis in HOS. Metastatic HOS cells expressed higher levels of F3 protein than non-metastatic cells and the quantification of F3 levels directly in human HOS patient samples showed that F3 was elevated in lung metastases relative to primary tumors. It has been demonstrated that F3 upregulation via the aberrant activation of its enhancers is required for lung colonization by metastatic HOS cells.	Morrow J.J. et al. 2018
CSF1	CSF1 and/or CSF-1R is important in regulating HOS cell EMT and metastasis. Theirs increased expression in HOS cells resulted in a highly significant increase in the invasiveness and mobility observed in vitro. In contrast, the CSF knockdown HOS cell had less invasiveness and mobility.	Wen Z. et al., 2017

SUPPLEMENTARY TABLES

Supplementary Table 1. List of Pediatric and adult sarcoma driver genes

geneID	Pediatric/Adult sarcoma	geneID	Pediatric/Adult sarcoma	geneID	Pediatric/Adult sarcoma
ALK	Pediatric sarcoma	CTNNB1	Adult sarcoma	RIOK2	Adult sarcoma
ARID1A	Pediatric sarcoma	EPHA1	Adult sarcoma	SETD2	Adult sarcoma
ATRX	Pediatric sarcoma	EPHA5	Adult sarcoma	STAG2	Adult sarcoma
BCOR	Pediatric sarcoma	EPHA7	Adult sarcoma	SYK	Adult sarcoma
BCORL1	Pediatric sarcoma	ERBB4	Adult sarcoma	TMEM60	Adult sarcoma
C10orf112	Pediatric sarcoma	EZH2	Adult sarcoma	TP53	Adult sarcoma
CTNNB1	Pediatric sarcoma	FANCA	Adult sarcoma	UNC50	Adult sarcoma
FLG	Pediatric sarcoma	FBXW7	Adult sarcoma	WRN	Adult sarcoma
HDAC2	Pediatric sarcoma	FLT4	Adult sarcoma		
KMT2D	Pediatric sarcoma	HGC6.3	Adult sarcoma		
LAPTM4B	Pediatric sarcoma	HRAS	Adult sarcoma		
MED12	Pediatric sarcoma	HS6ST1	Adult sarcoma		
NF1	Pediatric sarcoma	IDH1	Adult sarcoma		
NRAS	Pediatric sarcoma	IDH2	Adult sarcoma		
PDGFRA	Pediatric sarcoma	IRS1	Adult sarcoma		
PIK3CA	Pediatric sarcoma	KDM6A	Adult sarcoma		
PTEN	Pediatric sarcoma	KIT	Adult sarcoma		
RB1	Pediatric sarcoma	KRAS	Adult sarcoma		
RHOA	Pediatric sarcoma	LTK	Adult sarcoma		
ROS1	Pediatric sarcoma	MDC1	Adult sarcoma		
SIRPA	Pediatric sarcoma	MET	Adult sarcoma		
TP53	Pediatric sarcoma	MOS	Adult sarcoma		
ZMYM3	Pediatric sarcoma	MST1R	Adult sarcoma		
AKT1	Adult sarcoma	MUTYH	Adult sarcoma		
ASGR1	Adult sarcoma	MYOD1	Adult sarcoma		
ASXL1	Adult sarcoma	NF1	Adult sarcoma		
ATM	Adult sarcoma	NOTCH1	Adult sarcoma		
ATRX	Adult sarcoma	NRAS	Adult sarcoma		
BAP1	Adult sarcoma	NTRK1	Adult sarcoma		
BRCA2	Adult sarcoma	NUMA1	Adult sarcoma		
CDH1	Adult sarcoma	PDGFRB	Adult sarcoma		
CDKN2A	Adult sarcoma	PI4KA	Adult sarcoma		
CHEK2	Adult sarcoma	PIK3CA	Adult sarcoma		
CNPY3	Adult sarcoma	PLCG1	Adult sarcoma		
COL2A1	Adult sarcoma	PTCH1	Adult sarcoma		
CREBBP	Adult sarcoma	PTEN	Adult sarcoma		
PTK2B	Adult sarcoma	RB1	Adult sarcoma		
PTPRB	Adult sarcoma	RECQL4	Adult sarcoma		
PTPRT	Adult sarcoma	RET	Adult sarcoma		

Supplementary Table 2. List of Actionable Genes

geneID						
ABL1	CCNE1	ESR1	IGF2	MYCN	PIP5K1A	TET2
ABL2	CDK4	EZH2	JAK1	MYD88	PLCG2	TOP2A
AKR1B1	CDK6	FBXW7	JAK2	NCOR2	PML	TSC1
AKT1	CDKN1B	FGF3	JAK3	NF1	PRKCZ	TSC2
AKT2	CDKN2A	FGF4	KDR	NF2	PTCH1	TYK2
AKT3	CDKN2B	FGFR1	KIT	NOTCH1	PTEN	VEGFA
ALK	CDKN2C	FGFR2	KMT2A	NOTCH2	PTPN11	VEGFB
APC	CHEK2	FGFR3	LCK	NOTCH3	RAC1	YES1
AR	CSF1R	FGFR4	LYN	NOTCH4	RAD50	
ARAF	CSF3R	FH	MAP2K1	NPM1	RAF1	
ATM	CTNNB1	FKBP5	MAP2K2	NRAS	RARA	
ATR	DDR1	FLCN	MAP2K4	NTRK1	RET	
AURKA	DDR2	FLT1	MAP3K1	NTRK2	RICTOR	
AURKB	DNMT1	FLT3	MAP3K11	NTRK3	ROS1	
AURKC	DNMT3A	FLT4	MAP3K4	PALB2	RUNX1	
BAP1	DOT1L	FUS	MAP4K1	PDGFB	SLTM	
BCL2	EGFR	FYN	MAPK1	PDGFRA	SMARCB1	
BCR	EPHA1	GNA11	MAPK8	PDGFRB	SMO	
BRAF	EPHA2	GNAQ	MDM2	PGF	SMOX	
BRCA1	EPHA3	HDAC9	MET	PGR	SRC	
BRCA2	EPHA4	HGF	MGMT	PIK3C2B	STK11	
BTK	EPHB2	HRAS	MITF	PIK3CA	STK4	
CBFB	ERBB2	HSP90AA1	MMP2	PIK3CB	SYK	
CCND1	ERBB3	IDH1	MPL	PIK3CD	TAOK1	
CCND2	ERBB4	IDH2	MST1R	PIK3R1	TAOK2	
CCND3	ERCC2	IGF1R	MTOR	PIK3R2	TEK	

Supplementary Table 3. Deseq2 Differential Expression. List of up- and down-regulated gens in metastatic patients compared to localized patients (genes involved in the "Inflammatory Response_Hallmark" are reported in red)

gene_name	log2FoldChange	Status
CEACAM6	7.32341807314229	Up
SLC6A14	6.74691045512626	Up
SERPINB3	6.59250572995673	Up
ITGB6	5.97278847622961	Up
AC243967.1	5.91510486892728	Up
TMEM132C	5.15565011594508	Up
OR6N1	5.06580140610862	Up
TAC3	4.95659654822344	Up
RETN	4.92609821400587	Up
SLC4A1	4.72383024644424	Up
CTSE	4.59267343381912	Up
MCEMP1	4.49450956518031	Up
SOST	4.2929270792389	Up
FAT2	4.28782233053882	Up
MEPE	4.26758900155413	Up
OCSTAMP	4.12397718816312	Up
NOTO	4.04256486502923	Up
CD300LG	4.0397537693264	Up
PRSS22	3.89536083911013	Up
ITLN1	3.85890022592653	Up
HEMGN	3.84179473743295	Up
PDZK1IP1	3.83421866622662	Up
LIPH	3.80199858665048	Up
AADAC	3.70841968472904	Up
OR2W3	3.68174522770877	Up
IL6	3.60249686254626	Up
TNR	3.53595848330397	Up
PAQR9	3.49199177621598	Up
HBA1	3.4394439089475	Up
KLK11	3.43663976933068	Up
TACSTD2	3.41479812043341	Up
ALAS2	3.37459353937691	Up
ABCC8	3.35940223871789	Up
FCER2	3.32321354809305	Up
SLC30A3	3.2624736531188	Up
ANXA8L1	3.21261845893963	Up
AHSP	3.19092471476013	Up
P2RY2	3.17358656259069	Up
GGTLC1	3.17276645147455	Up
ADH1B	3.16065051255202	Up
KLK13	3.13321753570973	Up
AQP9	3.10987493404224	Up
SPIC	3.04729163033721	Up
IL1RN	3.04606163784174	Up
TRIM58	3.03223386367165	Up
ANXA8	3.00961414822616	Up
FAM166B	3.00153019460646	Up
NPY4R2	2.949239081691	Up
H3C14	2.94834293779234	Up
ADGRE3	2.93537035566752	Up
LCN2	2.9342903640749	Up
TLX1	2.93231541536356	Up
COL22A1	2.92821728624139	Up
CCDC60	2.91622331486956	Up
GP9	2.90547733169741	Up
ADIPOQ	2.90274075491684	Up
NTSR1	2.8813911649108	Up
PHEX	2.87756122453291	Up
NKG7	2.86326045602825	Up
HYAL4	2.86217430246791	Up
MMP8	2.84330828920669	Up
SMIM35	2.82611177343463	Up
ALOX15	2.82152289697981	Up
SUCNR1	2.82061077256833	Up
HP	2.81374187573057	Up
INSYN2B	2.78055693490447	Up
MAS1	2.77225109878064	Up
SNTN	2.75721063832124	Up
KCNE1B	2.74017118206477	Up
ANKRD18B	2.74016840453276	Up
ONECUT3	2.73640355748532	Up
DCSTAMP	2.72863510333525	Up
AC233723.1	2.72705141581617	Up

CCL15	2.71359125651439	Up
LYPD3	2.70929614217302	Up
SIGLEC15	2.70371501486237	Up
HBA2	2.68212604989641	Up
KLK4	2.68125061210082	Up
ANXA3	2.62525969753224	Up
PRF1	2.62480645078015	Up
RND1	2.62122165247736	Up
MMP9	2.6151042863929	Up
ARX	2.61201167622747	Up
FAM83F	2.60175651197085	Up
CES1	2.59823222261507	Up
SH3GL2	2.57592538412985	Up
DNAH10	2.57555383269043	Up
SPP1	2.5721862822543	Up
FABP4	2.52781704447181	Up
RIMS3	2.51829259888018	Up
SP6	2.51441361276281	Up
F5	2.5050761118341	Up
B3GNT3	2.50013525144216	Up
SLC32A1	2.49301085857052	Up
TAFA4	2.48624378943012	Up
CBLN1	2.47553880964548	Up
CEACAM1	2.46129286669987	Up
MFAP5	2.44403152805538	Up
KRT7	2.44227841821809	Up
CACNA1E	2.44194057912039	Up
LITAFD	2.44142265291265	Up
ST14	2.44088492407585	Up
ATP6V0D2	2.42654238514708	Up
KCNK3	2.42370441722662	Up
ACP5	2.41562117268625	Up
CLGN	2.41545140132229	Up
TMPRSS4	2.38550422831213	Up
CBLC	2.38459303059944	Up
IL11	2.37476821305916	Up
CHMP4C	2.36151794366892	Up
S100A9	2.36084327366134	Up
DRC7	2.35944956477341	Up
GABRP	2.35872849248795	Up
SLITRK2	2.35543630044298	Up

CD164L2	2.35238804899956	Up
KBTBD12	2.3504318648142	Up
DMRT1	2.3449615428899	Up
S100A8	2.34013481110568	Up
MT1A	2.3397470078709	Up
PRR36	2.33671505890874	Up
LRRN2	2.31022500162716	Up
WNT1	2.30745825693178	Up
OVOL1	2.30327052605857	Up
TF	2.28030290438343	Up
C16orf54	2.27953436959567	Up
LONRF2	2.27304580471975	Up
SPTA1	2.2570635518625	Up
BCL7B	2.25483044089759	Up
APOC2	2.25322908676477	Up
CD84	2.23263129095375	Up
PYGM	2.23197665223651	Up
PF4	2.22667160222359	Up
WIPF3	2.22010490581459	Up
TGM2	2.21762277554345	Up
H3C15	2.21747029445364	Up
APOC4-APOC2	2.21416094809679	Up
LILRA5	2.20993856892743	Up
EPCAM	2.20700160308938	Up
CCL3L3	2.20662491525742	Up
SLC4A10	2.19408041985367	Up
IL1R2	2.17175469390459	Up
RHOV	2.16623888912604	Up
LGALS12	2.15073536325071	Up
TFPI2	2.1367522125072	Up
AL049634.2	2.09409987181236	Up
ROPN1L	2.08895326004273	Up
PRR15	2.08270754217479	Up
PLAAT5	2.08253606397023	Up
NCR3	2.06532800077016	Up
ENTPD3	2.06195025007249	Up
LRG1	2.05862246925267	Up
HS3ST1	2.05589989104311	Up
OLR1	2.03445406414098	Up
MMP13	2.02802083580539	Up
IL1B	2.02557759244051	Up

SIGLEC14	2.02521955147312	Up
NLRC4	2.02267972523092	Up
ALOX5AP	2.01385345065791	Up
GPD1	2.01228042315476	Up
OSCAR	1.99263879047262	Up
PLAAT3	1.98114479713726	Up
CITED4	1.97896648412555	Up
SELP	1.97658191339607	Up
TNFRSF11A	1.97498231552339	Up
FBP1	1.97141560644582	Up
CALCR	1.96809300637441	Up
CCL3	1.96343834108519	Up
CA2	1.96024345158095	Up
C12orf54	1.95784188931727	Up
CORT	1.94656396099975	Up
NDRG4	1.94629711153677	Up
GADD45G	1.94470955822923	Up
CYFIP2	1.94389190087203	Up
SRGN	1.93440727910376	Up
SLC22A1	1.93294707538809	Up
SLC37A2	1.92537816698701	Up
TMEM52	1.92195097860908	Up
PTPRN2	1.91490666817317	Up
IL5RA	1.9116707502902	Up
CD1A	1.90876209693793	Up
LAPTM5	1.90244788803279	Up
CKB	1.90188172493022	Up
SPI1	1.90043813664846	Up
GNA15	1.89344217492171	Up
CST3	1.87623725713934	Up
F3	1.86606424509214	Up
CCRL2	1.86475276421764	Up
CPN2	1.85547311096388	Up
LGR6	1.83591777332808	Up
GSTM5	1.82864051677588	Up
AKAP6	1.82835082681908	Up
HYAL1	1.82549794205597	Up
SLC30A2	1.82547960507062	Up
RAC2	1.82383725098521	Up
TBXA2R	1.82194705588496	Up
ABCA3	1.81682798024495	Up

NRIP3	1.81057523877707	Up
TM4SF19-TCTEX1D2	1.81025039818216	Up
SLC9B2	1.80895385036963	Up
GPR150	1.79612110787017	Up
TRIM67	1.79187230826849	Up
SPTB	1.78420933722889	Up
H2BC7	1.78013503356661	Up
AC011479.2	1.76234522470572	Up
IGSF21	1.76076516696448	Up
ADAM8	1.75113201223124	Up
KIAA0040	1.75000590178911	Up
ADRB2	1.7393429369725	Up
N4BP3	1.7393342256521	Up
SUSD2	1.73853789281215	Up
PLEK2	1.73506110174932	Up
AQP3	1.73025683537946	Up
SLCO4A1	1.72803975167895	Up
AL353579.1	1.71927058713471	Up
PLEK	1.71847165400111	Up
IRF1	1.71391656804663	Up
CCR1	1.71187638208399	Up
PHACTR1	1.70878872589034	Up
ALDH1A2	1.69710823070336	Up
UCP2	1.69607962949295	Up
SIRPB1	1.68872863342458	Up
AC092111.3	1.68405300931638	Up
CLEC4A	1.67426579359765	Up
ITGAX	1.67365286819912	Up
MATK	1.65855257922436	Up
ITGB3	1.65789632028622	Up
LRRC10B	1.65238915873915	Up
BMP8B	1.6512314569786	Up
FCN3	1.6507528231622	Up
TMEM40	1.64761967095369	Up
ANPEP	1.64250302483886	Up
ABCG1	1.63650135470432	Up
LTF	1.63209601015874	Up
CD300C	1.62438599278436	Up
CREG2	1.60570906340509	Up
KCNK13	1.60196873616219	Up
C5AR1	1.60146845088909	Up

CASP5	1.60113960861729	Up
SNX10	1.59389299303312	Up
RILP	1.59056977687012	Up
ZNF385A	1.58595971645953	Up
IFI30	1.58433095613174	Up
PIK3AP1	1.58305149380893	Up
PTPN22	1.58283488527557	Up
11 ARL	1.57897104363057	Up
CCDC3	1.57729496594569	Up
ATP6V0C	1.57255708387145	Up
ZNF556	1.56722808459538	Up
BMP8A	1.56479491324045	Up
LRRC25	1.55292127998734	Up
AC068234.1	1.54636678150469	Up
CD300LB	1.54411879180108	Up
RHOF	1.53952133773026	Up
MRO	1.53776420414706	Up
ENPP1	1.53503287912234	Up
LAT2	1.53277092305602	Up
MTSS1	1.50854745739673	Up
TKT	1.50675281584019	Up
S100A3	1.50353941829456	Up
LYL1	1.48849468591739	Up
AC093525.2	1.48146237295889	Up
CDK18	1.47640506446353	Up
GYPC	1.47515360585937	Up
CD68	1.47301563633329	Up
GYG2	1.46828963800245	Up
RGS10	1.4664989885245	Up
NRGN	1.46268165239637	Up
HHEX	1.4495332002628	Up
CD300A	1.44187914993123	Up
SLC9A7	1.4313132969747	Up
TYROBP	1.40763853858827	Up
OPN3	1.4066924169097	Up
GALNT6	1.39410983143688	Up
FAM189A2	1.38663676176874	Up
BCL2L1	1.38112715893447	Up
CD4	1.37728235403333	Up
AMPD3	1.37620977680611	Up
ARRDC4	1.36988071051072	Up

ITGA2	1.36247258604037	Up
MYBL2	1.35796660626485	Up
PTPRE	1.3397923879382	Up
SLC45A3	1.33403656998885	Up
SEMA7A	1.32617903782514	Up
1 VNN	1.32117272735798	Up
STRADB	1.31100774111944	Up
ADGRE2	1.30900546112741	Up
PIM3	1.30890814081511	Up
MAPK13	1.3065066716068	Up
EHD1	1.29635756988278	Up
EOGT	1.28689285140432	Up
FRAT1	1.28428983393404	Up
DMTN	1.27360313835939	Up
EFHD2	1.27352044936857	Up
LONRF3	1.27331232004806	Up
ST6GALNAC4	1.27296402136322	Up
MPP1	1.24950862221532	Up
NCEH1	1.23963929536417	Up
SLC48A1	1.23328153163487	Up
CSF1	1.23298131616226	Up
GPR4	1.20863975509398	Up
OSTM1	1.20789070804372	Up
NFKBIE	1.20250214737915	Up
ME2	1.201563896778	Up
VASP	1.19427784082689	Up
PLBD1	1.19360927524791	Up
SLC16A6	1.19322444736381	Up
SLC16A7	1.19022074290274	Up
CXCL16	1.18316142711932	Up
WWC1	1.17474103642363	Up
FZD5	1.16679594846122	Up
SCARF1	1.16650269700579	Up
PHETA1	1.16396245267433	Up
MYO6	1.16100126525986	Up
XPR1	1.16068862698965	Up
NATD1	1.157968368269	Up
CACNA2D4	1.14085618429971	Up
TFRC	1.13868467957601	Up
SLC29A1	1.13295383085842	Up
FAM241A	1.12062263756099	Up

TRIM8	1.11746890117414	Up
KCNAB2	1.114346264828	Up
NOCT	1.11034850430258	Up
STEAP3	1.10843247108949	Up
GPSM3	1.10821435782308	Up
IRAK3	1.10577525580855	Up
CHML	1.09604796287308	Up
CDC42EP3	1.08187891879594	Up
SETD1B	1.0702688108357	Up
BCAR3	1.06384955979234	Up
TNIP1	1.05254033182948	Up
ORAI1	1.04550378638137	Up
MID1IP1	1.04374160400355	Up
GNPTAB	1.03654906311894	Up
UBALD2	1.03525453661641	Up
PITPNM2	1.02920623956764	Up
PTPRJ	1.02787042405931	Up
OPN1SW	-6.8606292732227	Down
COL9A1	-5.98422629308775	Down
FAM151A	-5.9017563005573	Down
CSMD3	-5.76510344586093	Down
ERICH6B	-4.86986237200913	Down
CDH7	-4.77021448594915	Down
MUC5B	-4.64930683516246	Down
OSTN	-4.45419394374387	Down
HRNR	-4.31250126760409	Down
CA9	-4.22515515259256	Down
JSRP1	-4.21707962619019	Down
FAM184B	-4.12484158159588	Down
NKX6-2	-4.09775608490219	Down
SERPINE3	-4.06828709036617	Down
GRID2	-4.03286994863972	Down
ABHD16B	-3.98962461784228	Down
GRIK1	-3.95954229527358	Down
CDH10	-3.94678163491906	Down
CLEC3A	-3.94317860316314	Down
PDE6C	-3.9380858913388	Down
SLC3A1	-3.91655238814749	Down
USH1C	-3.89894607480229	Down
SPDYE3	-3.83459964215848	Down
B4GALNT4	-3.82623283918926	Down

ANGPTL8	-3.81308843770375	Down
CNTN5	-3.79283634931711	Down
FAM166A	-3.75994395902083	Down
NCAM2	-3.73402518902976	Down
TMC3	-3.7140824453316	Down
ADCY2	-3.71095484275316	Down
KRT79	-3.70426075110435	Down
TDRD12	-3.65120487940292	Down
TREH	-3.64889683644995	Down
PTCHD1	-3.55595551609288	Down
LRFN5	-3.55401736115248	Down
ZMAT4	-3.54185697056364	Down
GABRA2	-3.52535423150962	Down
MSMP	-3.50787416309174	Down
GDA	-3.47999442019263	Down
TLDC2	-3.46701526159236	Down
CNTN3	-3.43736404833985	Down
SLC22A2	-3.40044988946712	Down
CLVS1	-3.38887177655003	Down
LDLRAD2	-3.33511258662697	Down
PRR33	-3.30739460488892	Down
COL9A3	-3.30656700797091	Down
KRT14	-3.30390480181313	Down
DNER	-3.3012196089185	Down
PCDH10	-3.29607623350913	Down
VWC2	-3.29263111362102	Down
LRRTM4	-3.26936183835597	Down
NLGN1	-3.26429345952526	Down
PCLO	-3.23135984276244	Down
JPH1	-3.22113620559429	Down
GALNT13	-3.2095805515237	Down
LRP1B	-3.19389391065889	Down
PCDH11X	-3.19353413342766	Down
CNTD1	-3.18818917834752	Down
SYT14	-3.18000385416679	Down
RSPO3	-3.1766598662591	Down
F7	-3.16266985578968	Down
NDST4	-3.14115564148749	Down
AMH	-3.13460303427186	Down
SBSPON	-3.11411469018747	Down
SIM1	-3.11365321627034	Down

PROM1	-3.1072612454313	Down
SPATA21	-3.09986548985161	Down
SORCS1	-3.09341621657735	Down
SCRG1	-3.08227144996976	Down
ASXL3	-3.0704866083547	Down
ADGRL3	-3.06353697348269	Down
FOXH1	-3.04295217236589	Down
DCC	-3.02333135356985	Down
VIL1	-3.0083230621626	Down
FRMD5	-2.97135392302197	Down
GJB2	-2.96869941684509	Down
CACNA1G	-2.94574622290227	Down
CAPN6	-2.93984574077056	Down
CDH3	-2.93378134324224	Down
USP6	-2.90833880853079	Down
CNTN1	-2.89740258313672	Down
SLITRK5	-2.88922104752022	Down
RORB	-2.87947660011685	Down
GRM7	-2.86867388263392	Down
LUZP2	-2.86701310963995	Down
PROX2	-2.86647322099047	Down
ATP6V1C2	-2.84888020483016	Down
BHLHE22	-2.82914521511185	Down
CEND1	-2.81533454607403	Down
SULT4A1	-2.80865212505647	Down
COL2A1	-2.79757938713747	Down
SLITRK1	-2.78091012055727	Down
NEGR1	-2.77343055271998	Down
LMX1A	-2.75101208472693	Down
RGS8	-2.72809566215861	Down
CPA2	-2.69609169665636	Down
LINGO2	-2.69608851255998	Down
KSR2	-2.69589309662768	Down
MTMR7	-2.68969896860523	Down
KCNB2	-2.6864454722915	Down
CASQ1	-2.67624477631413	Down
SNX32	-2.65558855933746	Down
PTN	-2.64514537226505	Down
XPNPEP2	-2.64393111299689	Down
CPB1	-2.6374495990992	Down
GRIA2	-2.62945817078501	Down

MMP1	-2.61945500558158	Down
ST8SIA2	-2.61376197799653	Down
FOXP2	-2.60673227027221	Down
NDST3	-2.59264625615449	Down
EN2	-2.57507010164155	Down
UTS2B	-2.56264278367767	Down
DNAH8	-2.51894004588051	Down
SLC26A1	-2.51824233448803	Down
C2orf72	-2.47386139077782	Down
NEFM	-2.46206476652376	Down
RNF112	-2.42543171708739	Down
SCT	-2.42199721987482	Down
ABCB11	-2.41086860334946	Down
GRTP1	-2.40875719180623	Down
NTNG1	-2.39588471397273	Down
GRP	-2.38918978503405	Down
BRSK2	-2.34541751676826	Down
CRISPLD1	-2.33471378803134	Down
STRA6	-2.32656211448681	Down
TEKT5	-2.2819882358173	Down
C1QTNF7	-2.2759227531089	Down
TUBB2B	-2.27237455426054	Down
IGFL2	-2.25117729908343	Down
FLRT3	-2.24721100979284	Down
PLPPR4	-2.23482324066986	Down
C1QTNF3	-2.23043140098293	Down
SLC39A5	-2.22975351527797	Down
PDGFRL	-2.21293080248228	Down
PHACTR3	-2.20952534133219	Down
BCAS1	-2.20767237947127	Down
TSNAXIP1	-2.20166592455799	Down
PCDH20	-2.17543443896456	Down
AL592490.1	-2.1711503401939	Down
MTUS2	-2.15438745806135	Down
AC068775.1	-2.15186127915661	Down
S100A1	-2.14348554381941	Down
AIRE	-2.1429370981533	Down
C12orf60	-2.13683473494075	Down
EPHA5	-2.13594727724568	Down
CARD14	-2.13198144732849	Down
METTL11B	-2.12481960266607	Down

LRRN4CL	-2.12357642629732	Down
FOXJ1	-2.08888517453657	Down
WDR83	-2.08666669464379	Down
CORIN	-2.08219922493121	Down
ATP2B2	-2.07737663181987	Down
TBC1D26	-2.07484832360514	Down
MRGPRF	-2.0701479713352	Down
CBLN4	-2.0618441969852	Down
EEF1A2	-2.05665102562254	Down
HR	-2.04752835610715	Down
ADAMTS13	-2.04045786847416	Down
SCX	-2.03356536002149	Down
EFNB3	-2.02918820007977	Down
CACNA1I	-2.02767811265861	Down
COL8A2	-2.00452181417191	Down
MKX	-1.99766717513465	Down
ERICH2	-1.9935760434843	Down
AHNAK2	-1.99287594439709	Down
ST6GALNAC5	-1.97528148867062	Down
ABTB2	-1.97350059793564	Down
NKD2	-1.97205455071637	Down
HMCN1	-1.9716603342227	Down
ATP2B3	-1.96315108730163	Down
FAM177B	-1.95405660821057	Down
SOX5	-1.95280567778248	Down
PPFIA4	-1.94782502065101	Down
LRRN3	-1.94492174458496	Down
RGPD2	-1.93323231271277	Down
TOX	-1.92620333148717	Down
CRMP1	-1.91616167596413	Down
NINL	-1.9153471617514	Down
P4HA3	-1.90275443522497	Down
CCDC151	-1.90156389789248	Down
LGI2	-1.89439703954303	Down
CXCL14	-1.8924195016921	Down
SERHL2	-1.89094455349008	Down
PDPN	-1.87551307158348	Down
ENO2	-1.87476965520049	Down
CES4A	-1.85737528910544	Down
AHRR	-1.85580655119845	Down
HAPLN1	-1.84532441347282	Down

PLCD4	-1.82633682534033	Down
HSF4	-1.79979796153142	Down
ANGPTL2	-1.79021172574953	Down
MROH8	-1.76556609380066	Down
TLL1	-1.75978373544994	Down
SMOC2	-1.73845286503155	Down
RAP1GAP	-1.73479796324786	Down
DSEL	-1.72233032296979	Down
COL7A1	-1.71409187162938	Down
IGSF10	-1.69949956565799	Down
LRIG3	-1.69881308274602	Down
MMP2	-1.67423103751631	Down
C1QTNF2	-1.65682055848798	Down
C12orf73	-1.65237091312672	Down
LRRC66	-1.65186214383962	Down
SOX9	-1.64003425386683	Down
P2RX6	-1.63131548882893	Down
NFATC4	-1.62847617276325	Down
MATN1	-1.62224894878571	Down
PAPLN	-1.61468836371845	Down
AXIN2	-1.61087302371041	Down
C1QTNF3-AMACR	-1.60386771084454	Down
SFRP4	-1.60215507898499	Down
IL11RA	-1.59496097798057	Down
SERPINI1	-1.58609100939666	Down
AC005324.4	-1.57960708341981	Down
GID4	-1.5717358408445	Down
FIBIN	-1.55938880557456	Down
RGMA	-1.55393267531469	Down
MFAP2	-1.53278453002453	Down
NACAD	-1.52958138038562	Down
SLC25A48	-1.51701687106354	Down
GOLGA6L10	-1.51550234506871	Down
AC004805.1	-1.50788071032887	Down
FOXO3B	-1.50176281666892	Down
TPM2	-1.4939229462452	Down
STXBP6	-1.48931898623352	Down
TRIM16L	-1.47805389262601	Down
AC074143.1	-1.47544028855304	Down
IZUMO4	-1.46252762855487	Down
PRPSAP2	-1.46046314091912	Down

TUBG2	-1.43893521804599	Down
ZSWIM7	-1.42725976722014	Down
CFH	-1.42084966222208	Down
POP4	-1.42065682362948	Down
COL3A1	-1.42038942252589	Down
PIGL	-1.4084486621343	Down
PDCD5	-1.40436694095404	Down
TMEM225B	-1.39379826939134	Down
ZNF521	-1.38052978435177	Down
CFAP44	-1.37301038350284	Down
AJM1	-1.37069389712971	Down
AKAP3	-1.36976336962736	Down
PDZRN3	-1.35862352535302	Down
MAMDC4	-1.35739543569886	Down
PDE3A	-1.35029039001182	Down
CCDC85A	-1.34407827134292	Down
ADGRB2	-1.34218212556853	Down
TTC19	-1.32432918849705	Down
PHLDB2	-1.31821936691368	Down
WWP2	-1.28887123374295	Down
NOL3	-1.28699443969326	Down
AVIL	-1.27910167789248	Down
PPP1R3G	-1.2784397309153	Down
DRG2	-1.26940338619739	Down
C19orf12	-1.26579960101396	Down
PNN	-1.25954671251173	Down
LRRC75B	-1.25422105121562	Down
PCID2	-1.24531904326003	Down
DRC3	-1.24237997200122	Down
C2orf74	-1.24181147901254	Down
SMARCD3	-1.23675157180045	Down
CNTNAP1	-1.22339151313163	Down

EGFR	-1.22185114390989	Down
PSMC3IP	-1.20638796490656	Down
CNTROB	-1.20526532793225	Down
SPTLC3	-1.2012179422924	Down
ULK2	-1.16997284074945	Down
ZNF337	-1.16866770003925	Down
GLT8D2	-1.16850939756001	Down
KRI1	-1.15898229035946	Down
WDR60	-1.14123500331363	Down
CLBA1	-1.13317834644886	Down
CLTCL1	-1.12880224029699	Down
SEM1	-1.11751566596581	Down
MPHOSPH8	-1.09280159405836	Down
IFI27L1	-1.08588739940922	Down
KAT2A	-1.08290758606742	Down
SH3BGR	-1.08075838160824	Down
TOP3A	-1.07208769409438	Down
LEO1	-1.0677019415332	Down
GOLGA2	-1.06042732797394	Down
PTGES3L-AARSD1	-1.05745388818546	Down
MED9	-1.04899743395975	Down
B9D1	-1.03889926834204	Down
AARSD1	-1.02708870098265	Down
RAD52	-1.02562076609065	Down
MTERF2	-1.02257763252886	Down
CALD1	-1.01781528851869	Down
2 NPR	-1.01141516134933	Down
TFB1M	-1.00739033330063	Down
SESN2	-1.00518272865407	Down
NBPF20	-1.00095907543719	Down